2008

Probing the Peptidyl Transferase Center of Ribosomes Containing Mutant 23s rRNA with Photoreactive tRNA

Nicole C. Caci
University of Massachusetts Amherst

PROBING THE PEPTIDYL TRANSFERASE CENTER OF RIBOSOMES CONTAINING MUTANT 23S rRNA WITH PHOTOREACTIVE tRNA

A Thesis Presented

by

NICOLE CACI

Submitted to the Graduate School of the
University of Massachusetts Amherst in partial fulfillment
of the requirements for the degree of

MASTER OF SCIENCE

February 2008

Biochemistry

PROBING THE PEPTIDYL TRANSFERASE CENTER OF RIBOSOMES CONTAINING MUTANT 23S rRNA WITH PHOTOREACTIVE tRNA

A Thesis Presented
by

NICOLE CACI

Approved as to style and content by:

_____
Robert A. Zimmermann, Chair

_____
Stephen S. Hixson, Member

_____
Molly Fitzgerald-Hayes, Member

_____
Danny J. Schnell, Department Head
Biochemistry and Molecular Biology

DEDICATION

To my parents, Janice and Nicholas Caci.

ACKNOWLEDGEMENTS

I would like to thank my advisor, Robert Zimmermann, for his thoughtful guidance and encouragement throughout this project. I appreciate the invaluable opportunity I have had to work with him. I would also like to extend my gratitude to Stephen Hixson for his helpful ideas and comments, and to Molly Fitzgerald-Hayes for her support during this project and throughout my years at the University.

I wish to express my thanks to all the members of the Zimmermann laboratory, especially Anton Manuilov, whose assistance was instrumental to this project, and Mona Gupta, for her helpful discussions and creative ideas.

A special thank you to my husband, parents, sister, and the rest of my family and friends. Their constant love and encouragement kept me going.

ABSTRACT

PROBING THE PEPTIDYL TRANSFERASE CENTER OF RIBOSOMES CONTAINING MUTANT 23S rRNA WITH PHOTOREACTIVE tRNA

FEBRUARY 2008

NICOLE CACI, B.S., UNIVERSITY OF MASSACHUSETTS

M.S., UNIVERSITY OF MASSACHUSETTS

Directed by: Professor Robert A. Zimmermann

There is strong crystallographic evidence that the 23S rRNA is the only catalytic entity in the peptidyl transferase center. Various mechanisms for the catalysis of peptidyl transfer have been proposed. Recently, attention has been given to the idea that the 23S rRNA simply acts to position the tRNA for spontaneous peptidyl transfer and that chemical catalysis may play only a secondary role. Conserved nucleotides U2585 and U2506 are thought to be involved in positioning the 3' ends of A- and P-site substrates based on the crystallographic evidence, and because mutagenesis at these sites severely impairs peptide bond formation. In this study, pure populations of ribosomes with either U2585A or U2506G mutations in the 23S rRNA were analyzed to test the hypothesis that substitutions at nucleotides U2585 and U2506 in the peptidyl transferase center impair peptide bond formation by altering the position of the 3' end of P-site tRNA relative to the 23S rRNA. Pure populations of mutant or wild-type ribosomes were obtained by an

affinity tagging system and probed with ^{32}P-labeled [2N_3A76]tRNA^{Phe} to determine how the 3' end of tRNA interacts with the ribosomal proteins and 23S RNA at the peptidyl transferase center. Some of the data for the ribosomes with a G at position 2506 are consistent with a model suggested by Schmeing and coworkers in which nucleotide U2506 breaks from its original wobble base pair with nucleotide G2583 during A-site tRNA binding and swings towards the 3' end of P-site tRNA, while nucleotide U2585 simultaneously moves away from the 3' end of P-site tRNA.

TABLE OF CONTENTS

ACKNOWLEDGEMENTS……iv

ABSTRACT……v

LIST OF TABLES……..ix

LIST OF FIGURES……x

LIST OF ABBREVIATIONS……xi

CHAPTER

1. INTRODUCTION……...1

2. MATERIALS AND METHODS……...13

Enzymes……...13
Chemicals and supplies……13
Buffers……..16
Growth of bacterial strains……...26

BL21(DE3) pGST-MS2……26
DH10 p278MS2……26

Ribosome preparation……..27

Purification of GST-MS2 fusion protein……..27
Preparation of 70S ribosomes……...29
Purification of MS2-tagged 70S ribosomes by chromatography…..30
Ribonuclease H analysis of MS2-tagged ribosomes…….31

Preparation of ^{32}P-labeled [2N_3A76]tRNA^{Phe}……..33

Labeling of p2N_3Ap with ^{32}P and ligation to tRNA^{Phe} lacking A76…….33
Purification of ^{32}P-labeled [2N_3A76]tRNA^{Phe} by gel electrophoresis……34

Binding and crosslinking of [2N_3A76]tRNA^{Phe} to 70S ribosomes……..35

Binding of [2N_3A76]tRNA^{Phe} to 70S ribosomes……..35
Crosslinking of [2N_3A76]tRNA^{Phe} to 70S ribosomes……...37
Isolation of crosslinked 50S subunits, 50S-subunit proteins, and 23S rRNA……...38

Analysis of crosslinking by gel electrophoresis……...39

Distribution of crosslinked tRNA between 23Sr RNA and 50S-subunit proteins……...39
Distribution of crosslinked tRNA among 50S-subunit proteins…...39
Partial localization of 23S rRNA crosslinks……40
Precise localization of 23S rRNA crosslinks……43

3. RESULTS……..49

Growth of bacterial strains……...49
Ribosome preparation……..52
Preparation of ^{32}P-labeled [2N$_3$A76]tRNA^{Phe}……..55
Binding and crosslinking……55
Collection of tRNA-ribosome complexes……59
Analysis of tRNA-ribosome complexes……..64
Analysis of tRNA-protein complexes……..64
Analysis of tRNA-23S rRNA complexes……66

Partial localization of 23S rRNA crosslinks……66
Precise localization of 23S rRNA crosslinks……79

4. DISCUSSION……84

BIBLIOGRAPHY……88

LIST OF TABLES

1. Characteristics of oligonucleotides used for RNase H and primer extension analysis…….15

2. Strain doubling times…….50

3. Binding and crosslinking of [$2N_3$A76]tRNA^{Phe} to wild-type and mutant ribosomes……..……...58

LIST OF FIGURES

1. Structure of the 23S and 5S rRNA in the 50S subunit of *H. marismortui*……..3

2. A proposed mechanism of peptide-bond formation…….4

3. Conserved nucleotides A2451, U2506, U2585, and A2602 are found close to the PTC……...6

4. Several nucleotides surrounding the PTC are flexible.……...8

5. Yeast $tRNA^{Phe}$ as a probe of the PTC of wild-type and mutant ribosomes.……11

6. Chimeric oligonucleotide-directed cleavage of 23S rRNA by RNase H……...42

7. Isolation of primer extension templates by preparative RNase H digestion.…….45

8. Expression of GST-MS2 fusion protein……....51

9. Purification of MS2-tagged ribosomes on GSTrap affinity columns……....53

10. Verification of purity of MS2-tagged ribosomes……...56

11. Labeling of $p2N_3Ap$ with ^{32}P…….57

12. Profile of radioactive material found in Nucleobond AX column fractions……..61

13. Fractionation of crosslinked ribosomal complexes by sucrose-gradient fractionation…….62

14. Distribution of crosslinks between 23S rRNA and 50S-subunit proteins……..65

15. Sequences to which oligonucleotides hybridize on 23S rRNA…….68

16. Analysis of tRNA-23S rRNA complexes by RNase H digestion……..69

17. Sequence to which chimeric oligonucleotides hybridize on 23S rRNA……....72

18. Analysis of tRNA-23S rRNA complexes by RNase H digestion using oligodeoxyribonucleotides and chimeric 2'-O-methyl/deoxyribonucleotides.74

19. Localization of radioactivity to regions of 23S rRNA……...78

20. Primer extension analysis of crosslinked 23S rRNA…….81

LIST OF ABBREVIATIONS

ADP	adenosine 5’-diphosphate
AMP	adenosine 5’-monophosphate
APS	ammonium persulfate
ATP	adenosine 5’-triphosphate
BSA	bovine serum albumin
CIAP	calf intestinal alkaline phosphatase
d.d. H_2O	double distilled water
DNase	deoxyribonuclease
DTT	dithiothreitol
EDTA	ethylenediaminetetraacetate
GST	glutathione S-transferase
HEPES	N-2-hydroxoxyethylpiperazine-N’-2-ethane-sulfonic acid
IPTG	isopropyl-β-D-thiogalactoside
LB	Luria-Bertani
LPA	linear polyacrylamide
MWCO	molecular weight cut-off
nt	nucleotides
oligo	oligonucleotide
OPA	one-phor-all
PAGE	polyacrylamide gel electrophoresis
PEG	polyethylene glycol
PEI-TLC	polyethyleneimine cellulose thin-layer chromatography
Phe	phenylalanine
$p2N_3Ap$	2-azidoadenosine bisphosphate
PNK	polynucleotide kinase
PNP	purine nucleoside phosphorylase
PPase	pyrophosphatase
PS-CTA	polystyrene-cellulose triacetate
psi	pounds per square inch
PTC	peptidyl transferase center
RNase	ribonuclease
rpm	revolutions per minute
SDS	sodium dodecyl sulfate
TBE	tris-borate-EDTA
TEMED	N,N,N’,N’-tetramethylethylenediamine
tris	tris(hydroxymethyl)aminomethane
TTGP	tri/tri glycerol-enhanced polyacrylamide
UV	ultraviolet

CHAPTER 1

INTRODUCTION

Ribosomes are complex ribonucleoproteins composed of two distinct yet cooperative subunits that direct the translation of mRNA into protein. In prokaryotic cells, the small 30S subunit and the large 50S subunit interact to form the 70S ribosome. The two subunits work together to move the mRNA and tRNA substrates through the aminoacyl (A), peptidyl (P), and exit (E) sites of the ribosome. Aminoacyl-tRNA binds to the A site and accepts the peptidyl moiety of peptidyl-tRNA bound to the P site, to elongate the growing peptide chain. The deacylated tRNA then moves from the P site to the E site where it is released, and the new peptidyl-tRNA is translated to the vacated P site. The small 30S subunit, made of 16S rRNA and 21 ribosomal proteins, binds mRNA, and mediates the selection of tRNA ligands according to codon-anticodon interaction between mRNA and tRNA. The large 50S subunit, made of 23S rRNA, 5S rRNA, and 34 ribosomal proteins, promotes peptide bond formation via an attack of the amino group of the incoming aminoacyl-tRNA upon the acyl group that links the growing peptide to the tRNA at the P site, at its peptidyl transferase center (PTC). In order to fully understand how protein synthesis occurs, the mechanism of catalysis at the PTC active site must be characterized.

Biosynthesis is typically assisted by enzymatic reactions between catalytic proteins and their substrates. However, it has been proposed that the 23S rRNA serves as a ribozyme at the PTC, and that the proteins present in the 50S subunit may simply help to fold and stabilize the three-dimensional structure of the rRNA (Ban et al., 2000). A high-resolution crystal structure of the 50S subunit from the archaeon *Haloarcula*

marismortui reveals that the active site of the PTC is composed of highly conserved nucleotides of 23S rRNA domain V **(Figure 1)**, and that there are no ribosomal proteins within 18 Å of the reaction site (Ban et al., 2000). The findings from the *H. marismortui* crystal structure support the hypothesis that the only catalytic entity in the peptidyl transferase reaction is the 23S rRNA (Ban et al., 2000). The ribosome structures of archaea and bacteria are similar, suggesting that this might also be the case in *Escherichia coli*, although there is also evidence for the presence of a protein at the *E. coli* PTC (Maguire et al., 2005).

One proposed mechanism of peptide bond formation suggests that the acid-base properties of nucleotide A2451 promote nucleophilic attack, linking the α-amino group of the A-site substrate and the acyl group of the P-site substrate **(Figure 2)** (Nissen et al, 2000). This mechanism is seen as involving specific nucleotides at positions A2451 and G2447, and implies that mutations there would be lethal. However, various studies reveal that ribosomes with mutations at A2451 and G2447 maintain a significant level of peptidyl transferase activity (Polacek et al., 2001; Thompson et al., 2001), and a 3-Å crystal structure of the *H. marismortui* 50S subunit containing A- and P-site substrates reveals that the P-site tRNA is unlikely to interact with A2451 in the manner proposed (Hansen et al., 2002). Additionally, in contrast to *H. marismortui* ribosomes, *E. coli* ribosomes contain a protein, L27, at the PTC. Analysis of bacterial ribosomes suggests that the N-terminus of L27 resides within 3-4 Å of the reaction site, and that this protein is an integral component of the peptidyl transferase reaction center (Maguire et al., 2005, Selmer et al., 2006). It is possible that L27 functions to help position the tRNA

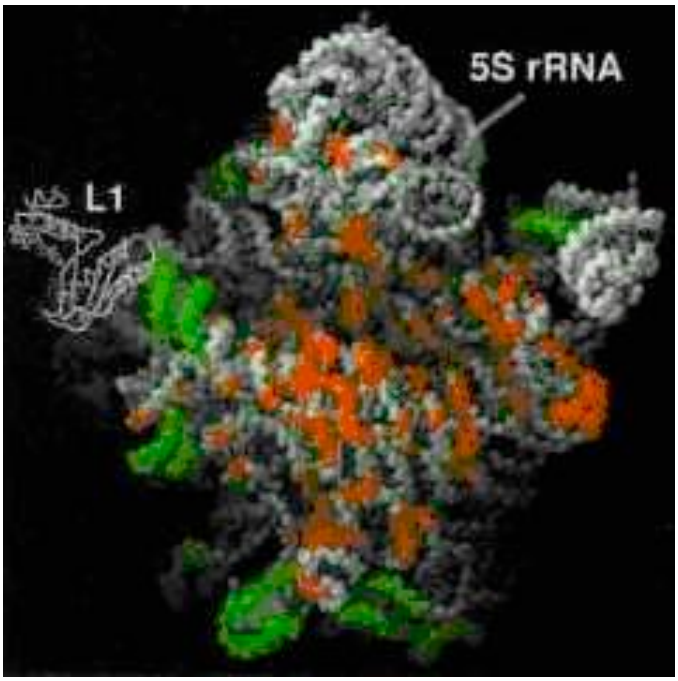

Figure 1. Structure of the 23S and 5S rRNA in the 50S subunit of *H. marismortui*. Highly conserved sequences (>95% across the three phylogenetic kingdoms) are shown in red, nonconserved sequences are shown in gray, and areas where expansion in the basic sequences are permitted are shown in green. From Ban et al., 2000.

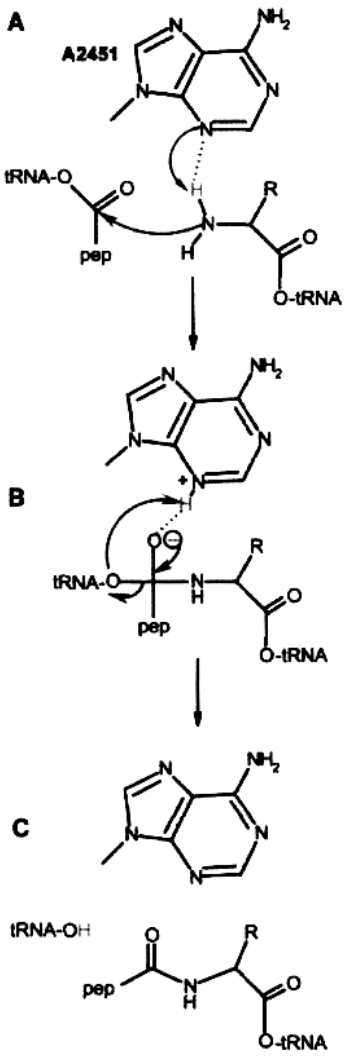

Figure 2. A proposed mechanism of peptide-bond formation. **(A)** The N3 of A2451 may form a hydrogen bond with the α-amino group of the A-site tRNA as the A-site tRNA attacks the carbonyl carbon of the P-site tRNA. **(B)** The protonated N3 bonds to the oxyanion of the substrate in its transition state, then **(C)** the proton is transferred to the P-site tRNA. From Nissen et al., 2000.

molecules at the PTC via its flexible N-terminus. Taken together, the findings discussed above suggest that the primary purpose of the 23S rRNA is not acid-base catalysis, and that the crystal structure of the 50S subunit is insufficient to explain how structural changes in tRNA-ribosome interaction may facilitate peptidyl transferase activity. Attention is now being given to the idea that the correct alignment of the 3' ends of tRNA substrates in the PTC is the primary catalytic activity of the 50S subunit. Because aminoacyl-tRNA arrives at the A site in an activated form, it has sufficient energy to allow spontaneous peptidyl transfer when the two substrates are properly positioned (Polacek et al., 2001).

There is ample evidence that 23S rRNA is important for positioning the tRNA in the A and P sites. For example, the CCA ends of the tRNA substrates interact with 23S rRNA through base-pairing (Kim and Green, 1999; Samaha et al., 1995). In addition there are several other nucleotides implicated as having key roles in the PTC, that may help to position the tRNA. Among these, nucleotides A2451, U2506, U2585, and U2602 are universally conserved and, based on the crystallographic evidence, are close to the catalytic site **(Figure 3)** (Ban et al., 2000; Yusupov et al., 2001). Moreover, mutagenesis of these nucleotides is detrimental to ribosome function *in vivo* (Green et al., 1997; Polacek et al., 2001; Thompson et al., 2001; Youngman et al., 2005) and cells reliant on ribosomes with mutations at these sites are often not viable or exhibit impaired growth *in vivo* (Youngman et al., 2004). The deleterious effects could be due to the inability of the mutant 23S rRNA to properly position the peptidyl- or aminoacyl-tRNAs at their respective sites.

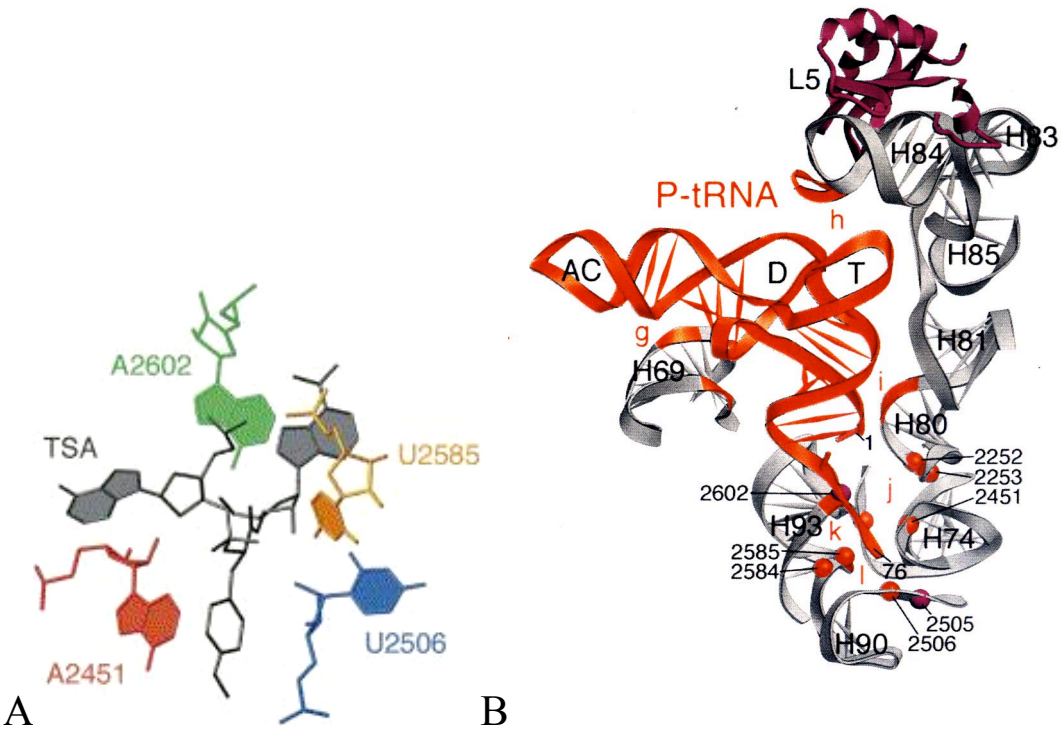

Figure 3. Conserved nucleotides A2451, U2506, U2585, and A2602 are found close to the PTC. **(A)** A crystallographic view of *H. marismortui* shows the nucleotides that surround a bound transition state analog, which represents the 3' ends of A- and P-site substrates during peptidyl transfer. From Youngman et al., 2004. **(B)** A full-length tRNA is shown interacting with the PTC while bound to the P-site of a *Thermus thermophilus* ribosome. From Yusupov et al., 2001.

Furthermore, there is flexibility and movement in several nucleotides surrounding the PTC as evidenced by disorder in the crystal structures (Schuwirth et al., 2005) inferred from a comparison of structures with different conformations (Korostelev et al., 2006; Schmeing et al., 2005, Schuwirth et al., 2005). In a 3.5 Å structure of the *E. coli* 70S ribosome, for instance, U2585 and U2602 are disordered, indicating that the region that surrounds the CCA ends of the tRNA is flexible (Schuwirth et al., 2005). In a comparison between the crystal structures of a *T. thermophilus* 70S ribosome complexed with deacylated P-site tRNA, and an *H. marismortui* 50S subunit complexed with a P-site CCA oligonucleotide, there is a significant difference in the positions of nucleotides A2451 and A2450 (**Figure 4A**) (Korostelev et al., 2006). Schmeing and coworkers have compared the PTC in several high resolution structures of the *H. marismortui* 50S subunit complexed with analogs of P-site, A-site and transition state substrates (Schmeing et al., 2005). They proposed a complex series of nucleotide movements as the ribosome changes from a state in which an A-site substrate has just bound to the ribosome (uninduced), to a state in which the P-site substrate is ready for nucleophilic attack by the A-site tRNA (induced), and finally to a transition state in which the reaction intermediate has been stablized (**Figure 4B**) (Schmeing et al., 2005). In the uninduced state, nucleotide G2583 interacts with U2506 via a wobble base pair, and U2585 interacts via van der Waals contact with the reactive ester group of the peptidyl tRNA (Schmeing et al., 2005). At the introduction of the A-site substrate, the complex moves into an induced state where nucleotide G2583 becomes displaced, which in turn causes its wobble basepair with U2506 to break, while U2506 swings 90° towards A76 of the P-site tRNA (Schmeing et al., 2005). The disruption also causes U2585 to shift away from A76 of the

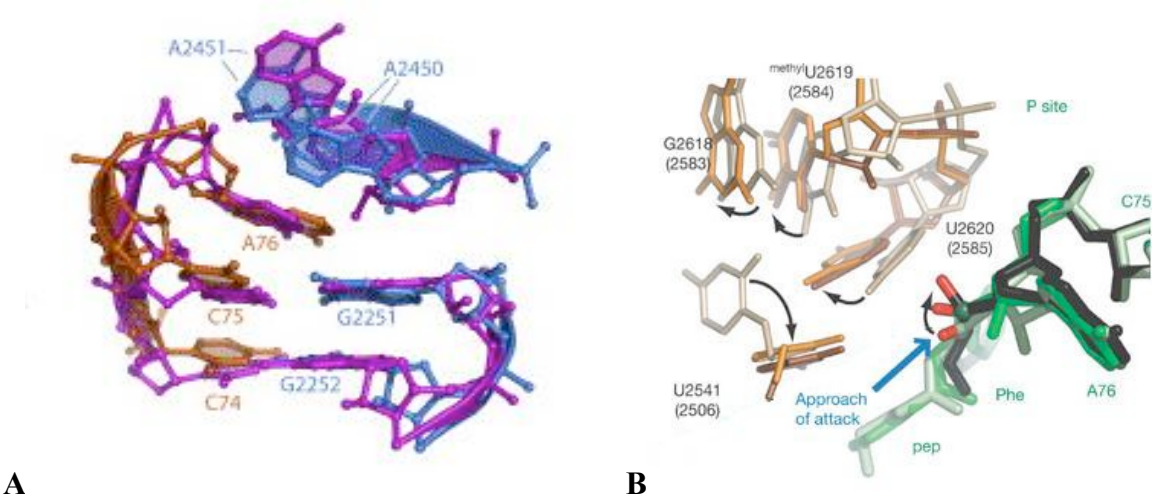

A **B**

Figure 4. Several nucleotides surrounding the PTC are flexible. **(A)** Comparison between the crystal structures of the *T. thermophilus* 70S ribosome (blue) complexed with deacylated P-site tRNA (orange), and the *H. marismortui* 50S subunit (magenta) complexed with a P-site CCA oligonucleotide (magenta). There is a significant shift in the positions of nucleotides A2451 and A2450, while the positions of other nucleotides including G2251 and G2252 remain unchanged. From Korostelev et al., 2006. **(B)** P-site-view overlay of three high resolution structures of the *H. marismortui* 50S subunit (wheat colors) complexed with analogs of P-site and transition state substrates (green and black). *E. coli* numbering is in parentheses. Schmeing et al. proposed a mechanism to explain how the ribosome changes from a state in which the A-site substrate has bound (uninduced) to a state in which the reaction intermediate is formed (transition state) (light to dark color). When the A-site substrate binds, the wobble basepair between nucleotides G2583 and U2506 breaks, and U2506 swings 90° towards A76 of the P-site tRNA. U2585 also shifts away from A76 of the P-site tRNA, leaving the P-site substrate open to attack from the A-site substrate. From Schmeing et al., 2005.

P-site tRNA towards that of the A-site tRNA, leaving the ester group of the P-site substrate open to attack from the A-site substrate, leading to the transition state (Schmeing et al., 2005). Investigation of how substitutions at these important 23S rRNA nucleotides may affect the interaction between the tRNA and the A and P sites is crucial to understanding the role of 23S rRNA in peptidyl transfer.

To test the hypothesis that substitutions at certain conserved nucleotides in the PTC impair peptide bond formation by altering the position of the 3' end of P-site tRNA relative to the conserved nucleotides, I have studied two kinds of mutant ribosomes, with either a U2506G or a U2585A substitution, by a series of biochemical analyses. The selection of these two positions was based on previous studies that have shown that the photoreactive nucleotide at the 3' end of the P site-bound substrate, $(2N_3A76)tRNA^{Phe}$, becomes crosslinked to both of these two nucleotides upon irradiation with UV light, suggesting that they are close to the PTC (Wower et al., 2000). The U2506G and U2585A mutations were chosen because of the severe decrease in the rate of peptidyl transfer observed in ribosomes carrying these substitutions (Youngman et al., 2004).

Pure populations of the mutated ribosomes were obtained by the use of an affinity tagging system. Plasmid p278MS2, provided by Elaine Youngman and Rachel Green (Johns Hopkins University), encodes the *E. coli rrnB* operon with a 23S rRNA gene engineered to contain a 35-nucleotide insert in the terminal loop of helix 98 (Youngman et al., 2004) where large insertions are tolerated (Spahn et al., 1999). The insert includes a 17-nucleotide affinity tag that can bind to the MS2 phage coat protein. Single nucleotide mutations have been introduced at positions U2506 and U2585 of the 23S rRNA gene within p278MS2 (Youngman et al., 2004). Expression of the mutant rRNA

genes is under control of the temperature-sensitive phage lambda repressor, cI857, encoded by the plasmid pcI857. Mutated ribosomes, including those with dominant-negative mutations, are expressed at levels as high as 50% (Youngman et al., 2004). Tagged p278MS2 wild-type and mutant ribosomes were purified away from normal ribosomes made in the same cells through their interaction with the MS2-domain of a GST-MS2 fusion protein immobilized on a glutathione sepharose column. Using the tagging system, the mutant ribosomes collected are more than 90% pure (Youngman et al., 2004). In all the experiments, ribosomes from wild-type MRE600 cells were used as controls.

The active sites of these ribosomes were studied using [5'-^{32}P](2N_3A76)tRNA^{Phe}, a radioactively-labeled tRNA^{Phe} whose 3'-terminal A residue has been replaced by a photoreactive 2-azidoadenosine residue **(Figure 5)** (Sylvers et al., 1989) labeled with a radioactive phosphate at the 5' position. The substrate binds primarily to the ribosomal P site and, when irradiated with 300-nm light, the photoreactive 3' adenosine forms 2- to 3-Å crosslinks to nearby proteins and nucleotides, thereby providing information about its proximity to the surrounding ribosomal components (Sylvers and Wower, 1993). It has been shown previously that this substrate forms crosslinks to protein L27, which is located near the active site, and to nucleotides U2585 and U2506 in the 23S rRNA upon excitation with UV light (Wower et al., 2000). In the present study, the crosslinking patterns generated by ^{32}P-labeled (2N_3A76)tRNA^{Phe} bound to the PTC of wild-type and mutant ribosomes were compared to examine whether the U2585A or U2506G mutations alter the crosslinking pattern which would indicate a change in the orientation of the 3' end of P-site tRNA relative to 50S-subunit components. Differences may point to the role

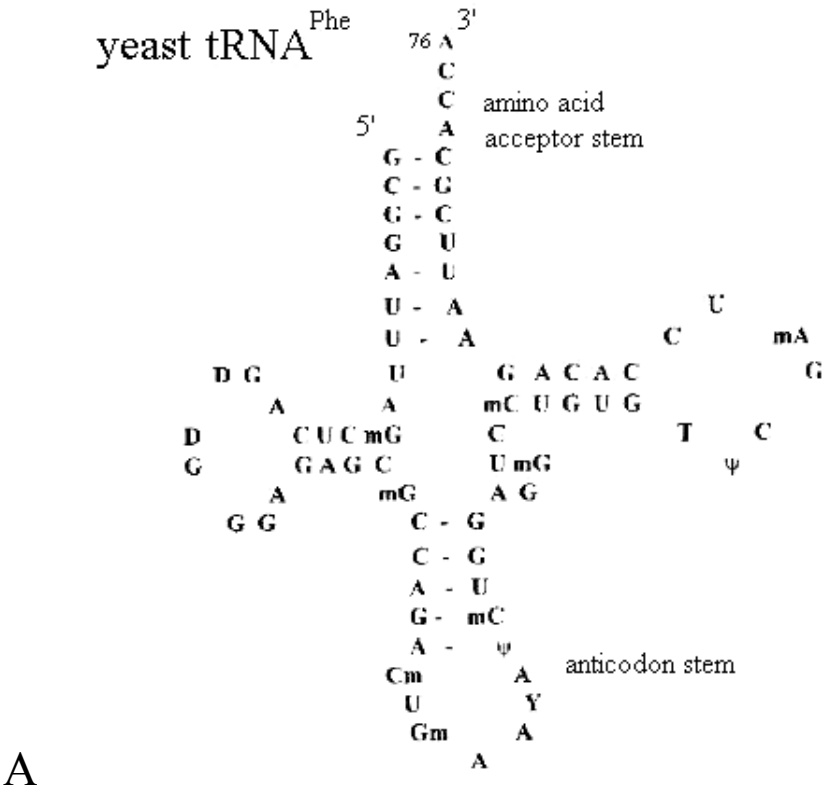

A

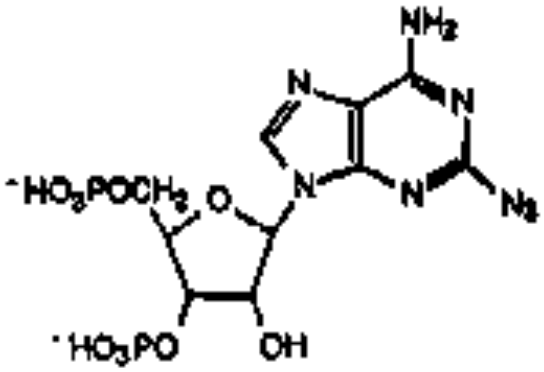

B

Figure 5. Yeast $tRNA^{Phe}$ as a probe of the PTC of wild-type and mutant ribosomes. **(A)** Secondary structure of yeast $tRNA^{Phe}$ (Baranovsky et al., 1997). **(B)** A photoreactive adenosine residue, 2-azidoadenosine bisphosphate, was labeled with ^{32}P at the 5' phosphate position then ligated to the 3' terminus of yeast $tRNA^{Phe}$ lacking A76 to generate ^{32}P-labeled $(2N_3A76)tRNA^{Phe}$ (Sylvers et al., 1989).

of 23S rRNA in positioning the tRNA for peptide transfer.The efficiency with which $(2N_3A76)tRNA^{Phe}$ bound and became crosslinked to each mutant ribosome, as well as the distribution of crosslinked ligand between 23S rRNA and 50S-subunit proteins, among individual 50S-subunit proteins, and among specific nucleotides of the 23S rRNA have been investigated. The results of several analyses in this study have been inconclusive. However, crosslink-localization data gained from primer extension and RNase H analyses are consistent with the model proposed by Schmeing et al. (2005) in which U2506 breaks from its original wobble base pair with G2583 and swings towards the A76 of P-site tRNA, while U2585 simultaneously moves away from the A76 of P-site tRNA during peptidyl-transfer (Schmeing et al., 2005, Figure 4B).

CHAPTER 2

MATERIALS AND METHODS

Enzymes

Hybridase thermostable ribonuclease H (RNase H) and T4 RNA ligase were purchased from Epicentre. Deoxyribonuclease I (DNase I), yeast pyrophosphatase (PPase) and purine nucleoside phosphorylase (PNP) were obtained from Sigma. 3' phosphatase-free T4 polynucleotide kinase (PNK) was purchased from Roche. S1 nuclease (100 U/μL), calf intestinal alkaline phosphatase (CIAP), and RNasin® Plus RNase inhibitor were produced by Promega. Avian Myeloblastosis Virus Reverse Transcriptase (AMV RT) was from Seikagaku.

Chemicals and Supplies

All inorganic reagents were purchased from Sigma-Aldrich Co., Fisher Scientific, or VWR. Yeast $tRNA^{Phe}$, bovine serum albumin (BSA), poly(U), adenosine 5'-diphosphate (ADP), glutathione sepharose, reduced L-glutathione, ammonium persulfate (APS), imidazole, inosine, β-mercaptoethanol, linear polyacrylamide (LPA), Coomassie blue (brilliant blue R), dithiothreitol (DTT), polyethylene glycol 8000 (PEG-8000), Triton X-100, kanamycin and ampicillin were purchased from Sigma-Aldrich Co. Difco Luria-Bertani (LB) Broth and Bacto Agar were obtained from Becton, Dickinson and Co. Glycerol and ethylenediaminetetraacetate (EDTA) were purchased from Acros/Organics, and glucose was bought from EM Industries, Inc. Alumina was obtained from Norton, and ultra-pure sucrose was purchased from ICN Biomedicals, Inc. Urea and bromophenol blue were from Fisher Scientific. Isopropyl-β-D-thiogalactoside (IPTG) was purchased from Calbiochem, and guanidine hydrochloride was obtained from

Applichem. [γ-^{32}P]ATP (specific activity 6000 Ci/mmol) was from Perkin-Elmer. Tricine, HEPES and acrylamide:*N,N,N',N'-bis*-acrylamide mixture (19:1, w/w) were purchased from Amresco Inc. SYBR gold was purchased from Molecular Probes. Sodium dodecyl sulfate (SDS) and N,N,N',N'-tetramethylethylenediamine (TEMED) were obtained from Boehringer-Mannheim Biochemicals. Xylene cyanole was from Eastman Kodak Co., Bio-Rad protein assay solution was from Bio-Rad Laboratories, and RNAsecure Reagent was from Ambion. Adenosine 5'-triphosphate (ATP) was purchased from Epicentre. DNA oligodeoxyribonucleotide and chimeric 2'-*O*-methyl oligonucleotide primers **(Table 1)** were from Integrated DNA Technologies. 2-Azidoadenosine bisphosphate ($p2N_3Ap$) was previously synthesized in our lab (Sylvers et al., 1989).

Nucleobond AX-20 columns were purchased from BD Biosciences. GSTrap Fast Flow columns (5 mL) and MicroSpin G-25 columns were obtained from Amersham. Nitrocellulose filters (0.45 μm pore size), Amicon Ultra-15 filters, and Centricon YM-3 filters were from Millipore. LongLife gels (4-20%) were purchased from Gradipore, and dialysis tubing (MWCO 8,000) was obtained from BioDesign, Inc. PEI-TLC plates were bought from EMD Chemicals, and PS-CTA filters (122 μm) were purchased from Island Pyrochemical Industries.

BL21(DE3) pGST-MS2 and DH10 p278-MS2 and derivatives were the kind gift of Elaine Youngman and Rachel Green, Johns Hopkins University.

Table 1. Charicteristics of oligodeoxyribonucleotides and chimeric deoxyribonucleotides/ 2'-*O*-methyl nucleotides used for RNase H and primer extension analysis

	Oligonucleotide	Oligonucleotide sequence (5'-3')[a.]	Positions of complementary 23S rRNA nucleotides
DNA	1	AGGGAGAACTCATCT	2776-2790
	3	TCGCGTACCACTTTA	2563-2577
	3b	ACATCGAGGTGCCAA	2492-2506
	4	GTTATCCCCGGAGTA	2438-2452
	4a	GCTCGCGCCGTCACG	2354-2368
	5	ACTACCCACCAGACA	2229-2243
	6	ATGTTCAGTGTCAAG	2084-2098
	7	CTTCACAGCGAGTTC	2018-2032
	8	ATAGTTACGGCCGCC	1903-1917
	1612	GGTTTGGGGTACGAT	1598-1612
Chimeric	2678	GCGT**CCACUCCG**	2667-2678
	2630	CAGC**GCCCACGG**	2619-2630
	2599	CTCA**CGACGUUC**	2588-2599
	2576	CGCG**UACCACUU**	2565-2576
	2543	CTTG**GGACCUAC**	2532-2543
	2502	CGAG**GUGCCAAA**	2491-2502
	2447	CCCC**GGAGUACC**	2436-2447
	2368	GCTC**GCGCCGUC**	2357-2368
	2242	CTAC**CCACCAGA**	2231-2242
	2094	TCAG**UGUCAAGC**	2083-2094
	2055	GTCT**UGCCGCGG**	2044-2055
Primer	2179	GGGTGGTATTTCTTGGTCGG	2160-2179
	2579	GCTCGCGTACCACTTTAAATG	2559-2579
	2667	GGTCCTCTCGTACTAGGAGCTG	2646-2667

a. 2'-O-methylated nucleotides are labeled in bold

Buffers

$T_{10}M_6N_{30}SH_4$ (T-buffer):	10 mM Tris-HCl, pH 7.5
	6 mM $MgCl_2$
	30 mM NH_4Cl
	4 mM β-mercaptoethanol
Sucrose cushion buffer:	20 mM Tris-HCl, pH 7.5
	500 mM NH_4Cl
	10 mM $MgCl_2$
	0.5 M EDTA
	1.1 M sucrose

Glutathione sepharose (GS) column buffers

Lysis buffer:	20 mM Tris-HCl, pH 7.5
	150 mM KCl
	2 mM DTT
Loading buffer, pH 7.3:	140 mM NaCl
	3 mM KCl
	5.4 mM Na_2HPO_4
	1.8 mM KH_2PO_4
	pH adjusted with HCl
GS-elution buffer:	50 mM Tris-HCl, pH 8.0
	10 mM reduced glutathione

Storage buffer, pH 7.3:	140 mM NaCl
	3 mM KCl
	5.4 mM Na_2HPO_4
	1.8 mM KH_2PO_4
	20% (w/v) glycerol
	pH adjusted with HCl

SDS-PAGE buffers

Tricine loading dye:	0.1 M Tris-HCl, pH 6.8
	0.18 M DTT
	4% (w/v) SDS
	20% (w/v) glycerol
	0.02% (w/v) bromophenol blue
Stacking gel:	0.72 M Tris-HCl, pH 8.45
	0.072% (w/v) SDS
	4% (w/v) 19:1 acrylamide:*bis*-acrylamide mixture
	0.001% (w/v) bromophenol blue
	0.1% (w/v) APS
	0.1% TEMED

Separating gel:	1 M Tris-HCl, pH 8.45
	0.1% (w/v) SDS
	10% (w/v) glycerol
	12% or 15% 19:1 acrylamide:*bis*-acrylamide mixture
	0.1% (w/v) APS
	0.1% TEMED
Upper running buffer:	100 mM Tris
	100 mM Tricine
	0.1% (w/v) SDS
Lower running buffer:	100 mM Tris-HCl, pH 8.9
Fairbanks A solution:	0.05% (w/v) Coomassie blue
	25% (v/v) isopropanol
	10% (v/v) acetic acid
RNase-away:	5% H_2O_2
	0.1% (w/v) SDS
	50 mM NaOH

GSTrap buffers

Binding buffer:	20 mM Tris-HCl, pH 7.5
	100 mM NH_4Cl
	10 mM $MgCl_2$
70S-elution buffer:	50 mM Tris-HCl, pH 7.5
	100 mM NH_4Cl
	10 mM $MgCl_2$
	10 mM reduced glutathione

Nucleobond AX column buffers (rRNA)

AX-extraction buffer:	100 mM Tris acetate, pH 6.3
	0.5 M KCl or NaCl
	15% (v/v) ethanol
	0.01% (v/v) Triton X-100
	6 M urea
AX-bind buffer:	50 mM Tris acetate, pH 6.3
	0.5 M KCl or NaCl
	15% (v/v) ethanol
AX-wash buffer:	50 mM Tris acetate, pH 6.3
	0.8 M KCl or NaCl
	15% (v/v) ethanol

AX-elute buffer:	50 mM Tris acetate, pH 6.3
	1.2 M KCl or NaCl
	15% (v/v) ethanol

RNase H buffers

Modifying buffer A (1X):	15 mM Tris-HCl, pH 7.8
	50 mM NH_4Cl
	1 mM Mg acetate
Modifying buffer B (1X):	10 mM Hepes-KOH, pH 7.0
	50 mM KCl
	0.1 mM EDTA
Enzyme dilution buffer (1X):	180 mM Hepes-KOH, pH 7.8
	45 mM KCl
	0.1% (v/v) Triton X-100
	2.25 mM $MnCl_2$

RNase H gel buffers

RNase H loading buffer (1X):	30 mM triethanolamine
	30 mM Tricine
	2.5 mM EDTA
	20% (v/v) glycerol
	0.1% (v/v) Triton X-100
	0.01% (w/v) xylene cyanole
	0.01% (w/v) bromophenol blue
TTGP gel:	30 mM triethanolamine
	30 mM Tricine
	2.5 mM EDTA
	10% (v/v) glycerol
	5% 19:1 acrylamide:*bis*-acrylamide mixture
	0.05% (w/v) APS
	0.1% (v/v) TEMED
Tri/Tri running buffer:	30 mM triethanolamine
	30 mM Tricine
	2.5 mM EDTA

Bisphosphate labeling buffer (1X):	50 mM imidazole, pH 6.6
	10 mM $MgCl_2$
	0.1 mM EDTA, pH 8.0
	1 mM inosine
	0.25 mM ADP
	5% (w/v) PEG-8000
Ligation buffer (1X):	80 mM HEPES, pH 7.5
	15 mM $MgCl_2$
	10 μM ATP, pH 7.0
	10 μg/mL BSA
Nucleobond AX column buffers (tRNA)	
AX-bind buffer:	50 mM Tris acetate, pH 6.3
	0.2 M NaCl
	15% (v/v) ethanol
AX-elute buffer:	0.6 M Na acetate, pH 8.0
	30% (v/v) ethanol
AX-flush buffer:	50 mM Tris acetate, pH 6.3
	1.5 M NaCl
	15% (v/v) ethanol

One-Phor-All (OPA) buffer:	10 mM Tris acetate, pH 7.5
	10 mM Mg acetate
	50 mM K acetate

tRNA purification and sequencing gel buffers

TBE (1X):	90 mM Tris
	90 mM boric acid
	2 mM EDTA
RNA loading dye:	0.03% (w/v) bromophenol blue
	0.03% (w/v) xylene cyanole
	6 M urea
	in 1X TBE
Polyacrylamide gel:	8% or 6% (w/v) 19:1 acrylamide:*bis*-acrylamide mixture
	7 M urea
	0.05% (w/v) APS
	0.1% (v/v) TEMED
	in 1X TBE

RNA extraction buffer:	0.5 M NH_4 acetate
	1 mM EDTA
	10 mM Mg acetate
	0.1% (w/v) SDS or Triton X-100
P-site binding buffer (1X):	50 mM Tris-HCl, pH 7.5
	0.1 M NH_4Cl
	20 mM, 10 mM, 0.1 mM, or 0 mM $MgCl_2$
S1 buffer:	0.05 M Na acetate, pH 4.5
	1 mM $ZnSO_4$
	0.1 M NaCl
	0.1% (w/v) SDS
	6 M urea
S1 dilution buffer:	8.0 mM Zn SO_4
	0.4% (w/v) SDS
Sucrose gradient buffer:	10 mM Tris-HCl, pH 7.5
	50 mM KCl
	0.25 mM $MgCl_2$
	7 mM β-mercaptoethanol
	15% or 30% (w/v) sucrose

Kinase buffer (1X):	500 mM Tris-HCl, pH 7.8
	100 mM $MgCl_2$
	100 mM DTT
	10 mM Spermine
	1 mg/mL BSA
	5% (w/v) PEG-8000
Hybridization buffer (1X):	50 mM K-Hepes, pH 7.0
	100 mM KCl
	1X RNA secure
Extension buffer (1X):	130 mM Tris-HCl, pH 8.5
	10 mM $MgCl_2$
	100 mM DTT
Precipitation buffer:	85 mM Na acetate
	0.8 mM EDTA
	70% (v/v) ethanol

Growth of bacterial strains

BL21(DE3) pGST-MS2: The GST-MS2 fusion protein consists of a glutathione-S-transferase domain and an MS2 phage coat protein domain (Youngman et al., 2004). *E. coli* BL21(DE3) cells containing the plasmid for the GST-MS2 fusion protein, pGST-MS2, were grown overnight on an LB agar plate with 1 g/L of glucose and 100 μg/mL of ampicillin at 37 °C. A 50-mL starter culture in LB medium with the same concentrations of glucose and ampicillin was inoculated with a single colony of BL21(DE3) pGST-MS2 and incubated overnight at 37 °C. From the starter culture, 20 mL were used to inoculate 1 L of pre-warmed LB medium with the same concentrations of glucose and ampicillin. This culture was grown in a shaking incubator at 37 °C until the OD_{600} reached 0.5-0.6.

At this point the culture was cooled to room temperature, protein expression was induced with 0.1 mM of IPTG, and the culture was moved to a room temperature shaker and incubated overnight. To check protein expression, samples of cells were taken prior to induction, 2 hrs post-induction, and 21 hrs post-induction, and subsequently analyzed by SDS-PAGE. The cells were chilled on ice and sedimented by centrifugation in a Sorvall GSA rotor at 4 °C for 15 min at 10,000 rpm. The cell pellets were then washed in T-buffer, centrifuged again for 20 min, and stored in pellet form at –20 °C after decantation of the supernatant.

DH10 p278MS2: Plasmid p278MS2 encodes the *E. coli rrnB* operon in which the 23S rRNA gene has been engineered to contain a 35-nucleotide insert in the terminal loop of helix 98 (Youngman et al., 2004). The insert includes a 17-nucleotide affinity tag that can bind to the MS2 phage coat protein. The rRNA operon in p278MS2 is under control of the temperature-sensitive phage lambda repressor, cI857, encoded by the

plasmid pcI857. Single nucleotide mutations have been introduced at positions A2451, U2506, U2585, and A2602 of the 23S rRNA gene within p278MS2 (Youngman et al., 2004). DH10 pcI857 cells containing p278MS2, p278MS2(U2506G), and p278MS2(U2585A) were grown overnight at 30 °C on LB agar plates with 1 g/L of glucose, 100 μg/mL of ampicillin, and 50 μg/mL of kanamycin. 50-mL starter cultures in LB medium with the same concentrations of glucose and antibiotic were inoculated with a single colony and incubated overnight at 30 °C. From the starter cultures, 20 mL were used to inoculate 1 L of pre-warmed LB medium, with the same concentrations of glucose and antibiotic. These cultures were grown in a shaking incubator at 42 °C until the OD_{600} reached 0.7-0.9. At 42 °C, the temperature-sensitive lambda repressor is inactivated, allowing expression of the engineered rRNA genes on p278MS2 and its mutant derivatives. The cultures were chilled on ice and then harvested as described above.

Ribosome preparation

Purification of GST-MS2 fusion protein: BL21(DE3) pGST-MS2 cell pellets were resuspended in 15-20 mL of pre-chilled lysis buffer. They were kept in an ice and ethanol bath, and lysed by sonication using a Bransan Sonifier with a microtip for 2 min at power level 6 and 50% duty cycle. To remove cell debris, the lysate was then centrifuged in a Sorvall SS-34 rotor for 15 min at 4°C and 10,000 rpm. The supernatant was next dialyzed against 1 L of pre-chilled loading buffer overnight at 4 °C. To further clarify the dialyzed lysate, it was centrifuged the following day in a Sorvall SS-34 rotor for 30 min at 4 °C and a speed of 12,500 rpm (up to 16,000 rpm).

A 2-mL glutathione sepharose (GS) column was prepared as described by the manufacturer and pre-equilibrated with 5 mL of loading buffer. At 4 °C, the clarified lysate was loaded onto the GS column and washed with 4 mL of loading buffer. The GST-MS2 fusion protein was eluted with 10-15 of GS-elution buffer and collected in 1-mL fractions. A Bio-Rad (Bradford) assay was performed on each elution fraction by adding 20 μL of sample to 1 mL of Bio-Rad reagent that was prepared according to the manufacturer's instructions. The A_{595} of each was measured and compared to a BSA standard curve to determine the relative protein concentration. Each fraction from the purification process, including the samples taken to monitor GST-MS2 protein expression (see above), were checked for the presence of the fusion protein by 12% SDS-PAGE.

To prepare the protein-expression samples for the gel, the cells were sedimented in a microfuge tube for 20 min at 14,000 rpm and resuspended in 200 μL loading buffer. A 5-μL portion of Tricine loading dye was added to 10 μL of the suspension. The column fractions were prepared by adding 5 μL of Tricine loading dye to 5-10 μL of each fraction, depending on their relative concentration of protein. To each sample, one grain of urea was added, followed by heating at 95 °C for 3 min. The samples were run with upper and lower running buffers at 100 V for 2-3 hrs until bromophenol blue reached the bottom. The gel was then stained with Fairbanks A solution and rinsed in 10% acetic acid.

All fractions containing the fusion protein were pooled and dialyzed against 1 L of storage buffer to remove the glutathione. After 6 hours, the storage buffer was replaced and dialysis was continued overnight. The concentration of fusion protein was

determined by the Bio-Rad protein (Bradford) assay using BSA as a standard. The fusion protein was supplemented with storage buffer to a final concentration of 1 mg/mL, and was stored at –80 °C in 1-mL aliquots.

Preparation of 70S ribosomes: Frozen DH10 p278MS2 cell pellets (~1 g) were thawed briefly on ice, and then transferred to an ice-cold mortar. They were lysed by grinding as approximately 2.5 g of alumina were slowly added. For most of the ribosome preparations, broken cells were rinsed with 15 mL of T-buffer. The first 2 mL of T-buffer contained 3 μg/mL of DNase I. The solution was then centrifuged at 4 °C in a Sorvall SS-34 rotor for 20 min at 10,000 rpm to remove unbroken cells and alumina. To remove fragmented cell envelope, the supernatant was transferred to SS-34 tubes cleaned with RNase-away, and centrifuged at 4 °C for 60 min at 12,500 rpm. This supernatant was then centrifuged for 18 hrs in a Beckman Ti 50.2 rotor at 4 °C and 17,000 rpm to sediment the ribosomes. For the final preparations of ribosomes, this procedure was altered in an attempt to increase the yield. Modifications included using a volume of 11 mL of T-buffer to rinse the lysed cells, while the final centrifugation step in the Beckman Ti 50.2 rotor involved layering the 11 mL of clarified lysate on top of 13 mL of sucrose cushion buffer and centrifuging at 34,000 rpm for 18 hr at 4 °C. These modifications were based on the method developed by Elaine Youngman and Rachel Green (Youngman and Green, 2005).

After centrifugation, the supernatant was discarded and the pellet was rinsed with 1 mL of cold binding buffer. Another 1 mL of binding buffer was added and a glass rod was used to gently break the pellet. The pellet was completely resuspended by slowly vortexing for 2 hr at 4 °C. The dissolved ribosomes were then transferred to 1.5-mL

microfuge tubes, and the Ti 50.2 tube was back-washed with 250 μL of binding buffer to minimize ribosome loss. The ribosome solution was then clarified by centrifugation at 4 °C for 5 min. The concentration of the 70S ribosomes was determined by A_{260} measurement where 1 A_{260} = 23 μM 70S ribosomes.

Purification of MS2-tagged 70S ribosomes by chromatography: To purify the MS2-tagged mutant ribosomes from the crude 70S ribosome mixture, a 5-mL GSTrap Fast Flow column (Amersham) was used at 4 °C. A pump maintained a constant flow rate of 0.5 mL/min. The column was pre-equilibrated with 5 mL of binding buffer and then loaded with MS2-GST fusion protein, which was thawed quickly in a room temperature water bath to avoid aggregation, at a 1:20 ratio of protein mass to the mass of crude ribosomes to be fractionated (5-8X molar excess of fusion protein over expected amount of tagged ribosomes). Typically, 3 mg of fusion protein was applied to the column for every 70 mg of crude ribosomes to be loaded, up to approximately 20 mg of protein. The column was washed with 5-10 mL of binding buffer, and then loaded with the crude 70S preparation diluted in 1-2 mL of binding buffer. Untagged ribosomes passed through unretarded. The column was washed with 25 mL of binding buffer. MS2-tagged ribosomes were eluted with 10-15 mL of 70S-elution buffer and 0.5-mL fractions were collected. After the columns had been used several times, they were washed with 6 M guanidine hydrochloride at room temperature to strip away contaminant build-up.

The A_{260} of each elution fraction was measured to determine the ribosome concentration. All of the fractions within the elution peak were pooled and then concentrated by centrifugation at 4,000 rpm and 4 °C in a 15 mL Amicon Ultra 100K

MWCO filter until the concentrate reached 200-150 μL (20-40 min). The final concentration of the ribosomes was determined by measuring the A_{260}. Aliquots were flash-frozen in liquid nitrogen and stored at –80 °C.

Ribonuclease H analysis of MS2-tagged ribosomes: Analysis with RNase H, which is an enzyme that cleaves the RNA in a DNA-RNA hybrid, was used to confirm the presence of the MS2 tag in the eluted ribosomes. The MS2 tag is part of a 35-nucleotide insert which replaces nucleotides 2797 to 2799 near the 3' end of the 23S rRNA, resulting in a net increase of 32 nucleotides relative to wild-type MRE600 23S rRNA. Oligodeoxyribonucleotide #1 **(Table 1)** hybridizes to 23S rRNA from nucleotides 2776 to 2790. This site is 114-129 nucleotides away from the 3' end of wild-type rRNA, and it is 146-161 nucleotides away from the 3' end of rRNA with an MS2 insert. Analysis by gel electrophoresis of RNase H degradation with oligonucleotide #1 reveals a larger fragment in digests of 23S rRNA encoded by p278MS2 plasmids (146-161 nt) compared to those of wild-type 23S (114-129 nt).

A 20-mL Nucleobond AX-20 column was used to isolate 23S rRNA from the mutant 70S ribosomes, as well as that of wild-type MRE600 rRNA that was previously prepared by our lab. The rRNA AX buffers containing KCl were used in the procedure. Two A_{260} units of ribosomes were thawed and mixed with 0.5 mL of AX-extraction buffer to dissociate the rRNA from the ribosomal proteins. The ribosomes were then loaded onto the column, which was pre-equilibrated with 3 mL of AX-extraction buffer. The empty tube was back-washed with 1 mL of AX-extraction buffer, which was also loaded onto the column. The column was washed twice with 2 mL of AX-extraction buffer. Urea was removed by washing the column twice with 2 mL of AX-bind buffer.

The column was then washed twice with 2 mL of AX-wash buffer to remove any remaining contaminants. To remove excess wash buffer, 120 µL of AX-elute buffer was passed through the column. Then, the 23S rRNA was eluted with two 600-µL aliquots of AX-elute buffer. The column was regenerated by passing through 4-6 mL of AX-elute buffer, 4-6 mL of d.d. H_2O, and finally 4 mL of 30% ethanol.

The two 600-µL fractions were each vortexed with 500 µL of room-temperature isopropanol and the 23S rRNA was precipitated after placing the tubes on ice for 15 min. The tubes were centrifuged at 4°C for 30 min at 14,000 rpm to sediment the RNA, and the supernatant was discarded. To rinse the pellet, 85% ethanol at room temperature was added carefully so as not to disturb the sediment. The sample was centrifuged again at 14,000 rpm for 5 min at room temperature, and the ethanol was removed. The tubes were left open on the bench for 1-2 min to permit evaporation of any remaining ethanol. The 23S rRNA was resuspended in d.d. H_2O by first resuspending the pellet in one tube in 15 µL, then transferring that suspension to the other tube. The rRNA concentration was determined by measuring the A_{260} of the solution.

From the suspension, 0.5 A_{260} units of 23S rRNA were added to 10 µL of RNase H modifying buffer A containing 10 µM of oligonucleotide #1, and 0.5 U/µL of RNase H. Control samples without the oligonucleotide were also prepared. Prior to addition of the enzyme, the oligonucleotide was hybridized to the rRNA by incubation in a MiniCycler thermocycler (MJ Research) with a heated lid at 55 °C for 3 min. Without removing the tubes from the thermocycler, the enzyme was added to each sample, and mixed by pipetting. The reaction was incubated for 15 min after which RNase H loading buffer was added and the mixture was chilled on ice. A 1.5-µL portion of 100X SYBR

Gold dye was also mixed in. The digests were then analyzed on a 5% TTGP gel, which was run at 10 W with Tri/Tri running buffer until the bromophenol blue reached the bottom (2.5 hrs).

Preparation of ^{32}P-labeled [2N_3A76]tRNA^{Phe}

Labeling of p2N_3Ap with ^{32}P and ligation to tRNA^{Phe} lacking A76: The 5' position of 2-azidoadenosine bisphosphate (p2N_3Ap) was labeled with ^{32}P using the exchange reaction catalyzed by PNK. The 10-μL labeling reaction contained 250 μM p2N_3Ap stock (A_{260}= 9.44 at pH 8.0, 1 mM), 12.5 μM of [γ-^{32}P]ATP, 25 U/mL of yeast PPase, 5 U/L of PNP, and 500 U/mL of 3' phosphatase-free PNK in bisphosphate labeling buffer. Prior to the addition of the PNK, the mixture was incubated at 37 °C for 30 min. After addition of the PNK, the mixture was again incubated at 37 °C for 30 min. After the incubation, the reaction mix was heated to 95 °C for 1 minute, and then chilled on ice.

A 0.5-μL sample was removed and diluted 1/1000 with sterile water. A 0.5-μL portion of this dilution was spotted onto a cellulose PEI-TLC plate, and the components were separated using 0.75 M KH_2PO_4, pH 3.5, until the solvent reached the top. The TLC plate was dried, covered with Saran wrap, and exposed to a phosphorimager screen. The percent of radioactivity that was incorporated into the p2N_3Ap was quantified by scanning the screen using a FLA-5000 phosphorimager (Fuji Medical Inc.), and analyzing the resulting data with Multi Gauge software (Fuji Medical Inc.), version 2.02.

The [5'-^{32}P]p2N_3Ap was then ligated to the 3' end of tRNA^{Phe} lacking A76 (Sylvers et al., 1989). The 625-μL reaction mix was comprised of 4 μM [5'-^{32}P]p2N_3Ap, 1 μM tRNA^{Phe}, 15% DMSO, 10 U/mL yeast PPase, and 320 U/mL T4 RNA ligase in

ligation buffer. This reaction was incubated at 4 °C for 19 hr. To remove excess proteins and other contaminants, the mixture was passed through a Nucleobond AX-20 column using the tRNA AX buffers. The sample was prepared for the column by diluting the reaction mixture to 1.25 mL with a final concentration of 150 mM Na acetate, pH 5.2, and 5% ethanol. It was then passed through the column, which was pre-equilibrated first with 2-3 mL of 30% ethanol, then with 2 mL of AX-bind buffer. The empty tube was backwashed with 1 mL of AX-bind buffer, which was then loaded onto the column. The column cartridge was washed four times with 2 mL of AX-bind buffer, then four times with 2 mL of 30% ethanol to remove salts. To remove excess ethanol, 120 µL of AX-elute buffer was passed through the cartridge. Then, the tRNA was eluted with four 500-µL aliquots of AX-elute buffer. The column was regenerated by washing with 4 mL of AX-flush buffer followed by 4 mL of 30% ethanol.

Each 500-µL fraction was supplemented with 9 µL of glacial acetic acid, 8.75 µL of 2.5 µg/mL LPA, and 725 µL of 100% ethanol. The tubes were placed at –80 °C for at least 30 min and the precipitate was sedimented by centrifugation at 4 °C for 30 min at 14,000 rpm. The pellets were gently washed with 200 µL of ice-cold 70% ethanol, and centrifuged again at 4 °C for 15 min at 14,000 rpm. The ethanol was removed, and the pellet was resuspended in 26.5 µL of d.d. H_2O.

Purification of ^{32}P-labeled [2N_3A76]tRNA^{Phe} by gel electrophoresis: The resuspended tRNA was incubated for 1 hr at 37 °C in a 30-µL solution containing OPA buffer, and 0.42 U/µL of CIAP. The sample was heated at 85 °C after the addition of 25 µL of RNA loading dye, and then chilled on ice. The tRNA was then loaded onto a pre-run 8% polyacrylamide gel and electrophoresed at 600 V, with TBE as a running buffer,

until the bromophenol blue reached the bottom. The gel was then exposed to a phosphorimager screen, which was scanned using the FLA-5000 phosphorimager. The radioactive band corresponding to the tRNA was excised and the tRNA was extracted in a foil-wrapped microfuge tube with 450 μL of RNA extraction buffer containing 0.01% Triton X-100. The gel was left to extract overnight on a rocking table.

The extracted tRNA was transferred to a fresh tube, and the empty tube was backwashed with 50 μL of RNA extraction buffer. In preparation for passage through a Nucleobond AX-20 column, the 500 μL of extracted tRNA were diluted to 1 mL by adding Na acetate, pH 5.2, to 150 mM, and ethanol to 5%. The tRNA was again subjected to AX column chromatography, and the eluted fractions were treated and precipitated as before. After centrifugation at 4 °C for 30 min, rinsing with 200 μL of ethanol, and recentrifugation for 15 min, the pellets were resuspended in a total of 20 μL of d.d. H_2O. The radioactivity was measured to determine the concentration of the tRNA.

In some cases, phenol/chloroform extraction was used to deproteonize the tRNA mixture in place of the Nucleobond AX-20 column. In these cases, the mixture was not diluted into Na acetate, pH 5.2 or ethanol, and the RNA extraction buffer contained 0.1% SDS instead of 0.01% triton X-100. The sample was extracted three times with phenol/chloroform (1:1 mixture of phenol/chloroform in Na citrate, pH 4.7), and then extracted two times with chloroform. Na acetate, ethanol, and LPA were then added, and the sample was precipitated with ethanol as in the Nucleobond AX procedure.

Binding and Crosslinking of [$2N_3$A76]$tRNA^{Phe}$ to 70S ribosomes

Binding of [$2N_3$A76]$tRNA^{Phe}$ to 70S ribosomes: [$2N_3$A76]$tRNA^{Phe}$ was prepared for the formation of non-covalent complexes with 70S ribosomes by heating in

a thermocycler with a heated lid at 65 °C for 5 min, cooling at room temperature for 10 min, then chilling on ice for 5 min. The ribosomes were activated by heating in the thermocycler for 5 min at 42 °C and then placed back on ice. The reaction mixture, which varied from 150 μL-1 mL (depending on the concentration of the tRNA preparation and the amount of crosslinked material desired), contained 0.15 μM [p2N_3A76]$tRNA^{Phe}$, 0.6 μM 70S ribosomes, and 2 A_{260}/mL of poly(U) in 20 mM $MgCl_2$ P-site buffer. The mixtures were pre-incubated at 37 °C prior to the addition of the tRNA and ribosomes. Once the ribosomes were added, the mixtures were incubated at 37 °C for 5 min to bind the poly(U) to the ribosomes. Then the tRNA was added and the incubation was continued at 37 °C for 15 min in the thermocycler with the heated lid, and then chilled on ice. To determine the amount of tRNA bound to the P-site of the 70S ribosomes, a filter-binding assay was used. Nitrocellulose filters with 0.45 μm pores trap ribosome-bound tRNA while allowing free tRNA to pass through.

In triplicate, 2.5 μL of the binding mixture was removed and mixed with 500 μL of cold 20 mM $MgCl_2$ P-site buffer in a microfuge tube. A control sample without 70S ribosomes was also prepared to determine the amount of background radioactivity that might result from nonspecific tRNA binding to the filters. The radioactivity of the 500-μL samples was measured in a scintillation counter. In later experiments, an additional 1 μL of the binding mixture was removed in triplicate, and the radioactivity of the pipet tip containing the sample was measured directly in the scintillation counter instead of measuring the 500-μL dilution. This was done to avoid any dissociation of the 50S and 30S subunits that might occur after dilution, prior to filtration, thereby affecting the results once the sample was applied to the nitrocellulose filters. With a vacuum of 7 psi,

the diluted samples were then applied to nitrocellulose filters that had been pre-soaked in 20 mM $MgCl_2$ P-site buffer. The filters were then gently washed with another 2 mL of 20 mM $MgCl_2$ P-site buffer. The radioactivity of the empty tubes was measured in the scintillation counter, and subtracted from the original radioactivity to determine the total amount of radioactivity that passed through the filters. The radioactivity bound to the dried filters was also measured in the scintillation counter, and the total percent of bound tRNA was determined.

Crosslinking of [2N_3A76]tRNA^{Phe} to 70S ribosomes: The tRNA-bound ribosomes were spotted (~10-20 μL per spot) onto plastic petri dishes, which were placed on ice and covered with a PS-CTA filter. PS-CTA filters reduce the transmittance of wavelengths below 300 nm and prevent the transmittance of wavelengths below 290 nm. The complexes were irradiated with 300-nm lamps for 5 min, and then transferred into a microfuge tube. The dishes were rinsed with 50 μL of 20 mM $MgCl_2$ P-site buffer to ensure maximum transfer of crosslinked material. DTT was added to a final concentration of 10 mM to stop the reaction. As in the assay for non-covalent tRNA-ribosome interaction, a filter-binding assay was conducted to determine the percent of tRNA crosslinked to the ribosomes. The filters used were pre-soaked in 0 mM $MgCl_2$ P-site buffer; triplicate 2.5-μL aliquots were diluted into 500 μL of 0 mM $MgCl_2$ P-site buffer, mixed gently, and passed through the filters. The filters were then rinsed in 0.1 mM $MgCl_2$ P-site buffer. Low concentrations of $MgCl_2$ were used to dissociate the 50S from the 30S subunits, releasing any uncrosslinked tRNA. The remaining samples were then precipitated with two volumes of ethanol at −80 °C for at least 1 hr. The samples

were centrifuged at 4 °C for 30 min and the pellets were resuspended in 100 μL of 0.1 mM $MgCl_2$ P-site buffer.

Isolation of crosslinked 50S subunits, 50S-subunit proteins, and 23S rRNA: The analysis of crosslinking by gel electrophoresis requires the isolation of 50S subunits and 23S rRNA. To isolate the 23S rRNA, a Nucleobond AX column was used. The same procedure for 23S rRNA isolation described earlier was followed, except that NaCl replaced KCl in the rRNA AX buffers to prevent precipitation of rRNA in SDS procedures. In this case, the flow-through containing crosslinked 50S-subunit proteins was also collected, and then concentrated to 200 μL by centrifugation in a SS-34 rotor at 7,000 rpm using a 2 mL Centricon YM-3 centrifugal filter device with a MWCO of 3,000. The concentrate was precipitated at –20 °C in 5 volumes of acetone, centrifuged for 30 min at 4 °C, and resuspended in 200 μL of d.d. H_2O. The protein was then re-precipitated with 5 volumes of acetone and centrifuged again. The pellets were resuspended in 10 μL of fresh S1 buffer. In some cases, the flow-through, mixed with the first 1 mL of wash buffer (~1.35 mL total), was saved for S1 treatment without undergoing the concentration procedure.

To isolate the 50S subunits, the crosslinked 70S ribosomes were loaded onto 15-30% sucrose gradients in gradient buffer. The 14 x 89 mm tubes had been pre-washed in RNase-away and rinsed in d.d. H_2O. The gradients were then centrifuged at 4 °C for 18 hrs at 28,000 rpm in a pre-chilled Beckman SW41 rotor. At the end of the centrifugation, the gradients were fractionated using an ISCO pump and absorbance detector. The radioactivity in the 0.5-mL fractions was measured in a scintillation counter, and those fractions corresponding to 50S subunits were pooled. $MgCl_2$ and Na acetate, pH 5.2

were added to the pooled samples to a final concentration of 0.01 M and 0.1 M, respectively. The samples were precipitated at –80 °C with two volumes of ethanol for at least 1 hr, centrifuged, and then resuspended in 200 μL of 10 mM $MgCl_2$ P-site buffer. They were re-precipitated at –80 °C with two volumes of ethanol for at least 1 hr, centrifuged, and resuspended in 20 μL of S1 buffer.

Analysis of crosslinking by gel electrophoresis

Distribution of crosslinked tRNA between 23S rRNA and 50S-subunit proteins: A 10-μL portion of the resuspended 50S subunits was used to determine the distribution of crosslinking between the 23S rRNA and 50S-subunit proteins. The samples were mixed with 5 μL of Tricine loading dye and heated for 3 min at 95 °C. They were then loaded onto a 4-20% LongLife gel (Gradipore). The gel was run at 20 mA per plate on a Mighty Small II SE 250 apparatus (Hoefer Scientific Instruments) with "upper" and "lower" running buffers for about 2.5 hrs, until the bromophenol blue reached the bottom. The gel was then dried, covered with plastic wrap, and exposed to a phosphorimager screen. The screen was then scanned using a FLA-5000 phosphorimager to determine the percentage of the tRNA crosslinked to proteins and 23S rRNA.

Distribution of crosslinked tRNA among 50S-subunit proteins: To determine the distribution of crosslinks among the 50S-subunit proteins L27 and L33, the crosslinked 50S subunits were digested with S1 nuclease. S1 nuclease digests all RNA, leaving only [5'-^{32}P]AMP-crosslinked proteins. S1 nuclease (final concentration 10 U/μL) was added to 10 μL of 50S ribosomes that were resuspended in S1 buffer from the sucrose-gradient fractions or to 10 μL of ribosomal proteins that had been concentrated from AX column flow-through. The reaction was incubated for 2 hrs at 37 °C, and then 5

μL of Tricine loading dye was added. In some cases the samples were heated to 95 °C for 3 min.

Approximately 1.35 mL of unconcentrated AX column flow-through was used as an alternative to the pre-concentrated flow-through during some experiments. In this situation, 0.45 mL of S1 dilution buffer and 17 μL of glacial acetic acid were added for a final volume of approximately 1.8 mL before adding S1 nuclease to a final concentration of 10 U/μL. The reaction of S1 with the unconcentrated AX column flow-through was incubated for 2 hr at 37 °C, concentrated by Centricon YM-3 centrifugal filter (Millipore) to approximately 200 μL, and the protein precipitated with 1 mL of acetone at -20°C for 1 hr. The sample was then centrifuged for 15 min at 4 °C, and the supernatant was decanted. The pellet was washed with 200 μL of cold 80% acetone and centrifuged for 15 min at 4 °C. The supernatant was removed and the pellet was resuspended in 20 μL of tricine loading buffer.

The samples, prepared from sucrose gradients or AX column flow-through, were loaded onto a 15% SDS-PAGE gel with "upper" and "lower" running buffers, and run for about 11 hrs at 350 V (200 V if overnight). After the first 7 hr, or when all the dye had run off the gel, more loading dye was added and the gel was allowed to run for another 4 hr, or until the second application of dye reached the middle of the plate. At the end of the run, the gel was treated and scanned as in the previous gel protocol.

Partial localization of 23S rRNA crosslinks: To determine the approximate locations of the tRNA crosslinks on the 23S rRNA, tRNA-23S rRNA complexes were cleaved into specific segments using RNase H in conjunction with a series of oligodeoxyribonucleotide primers complementary to specific sequences in 23S rRNA.

Because of problems with this protocol due to cleavage ambiguity and inadequate hybridization sites (see Results), the procedure was also carried out using a series of chimeric oligonucleotides containing blocks of deoxynucleotides and 2'-*O*-methyl nucleotides. Because RNase H specifically cleaves the RNA adjacent to the 5' end of such chimeric oligonucleotides, the cleavage sites are unambiguous, allowing for more accurate quantification (**Figure 6**). The chimeric oligonucleotides were also designed to bracket the proposed sites of crosslinking to avoid hybridization across the sites of tRNA attachment.

Each sample of Nucleobond AX-purified 23S rRNA was split into 10 µL reactions containing a minimum of 1,500 cpm per reaction. When oligodeoxyribonucleotide primers were used, the reaction mixes contained 0.5 A_{260} units of 23S rRNA (supplemented with cold 23S if needed) and 10 µM each of one or two oligonucleotide primers in RNase H modifying buffer A. Prior to addition of the enzyme, the primers were hybridized to the rRNA by incubation in a MiniCycler thermocycler (MJ Research) with a heated lid at 55 °C for 3 min. Without removing the tubes from the thermocycler, the RNase H was added to each sample to a final concentration of 0.5 U/µL. The samples were mixed by pipetting, then incubated for 15 min after which RNase H loading buffer was added and the mixture was chilled on ice. A 1.5-µL portion of 100X SYBR Gold dye was also mixed in. The digests were then analyzed on a 5% TTGP gel, which was run at 10 W with Tri/Tri running buffer until the bromophenol blue reached the bottom (2.5 hrs). The gel was scanned for SYBR Gold-fluorescent bands using a blue-fluorescent laser to determine the mass of each fragment. The gel was then dried, covered with plastic wrap, and exposed to a phosphorimager screen. The screen

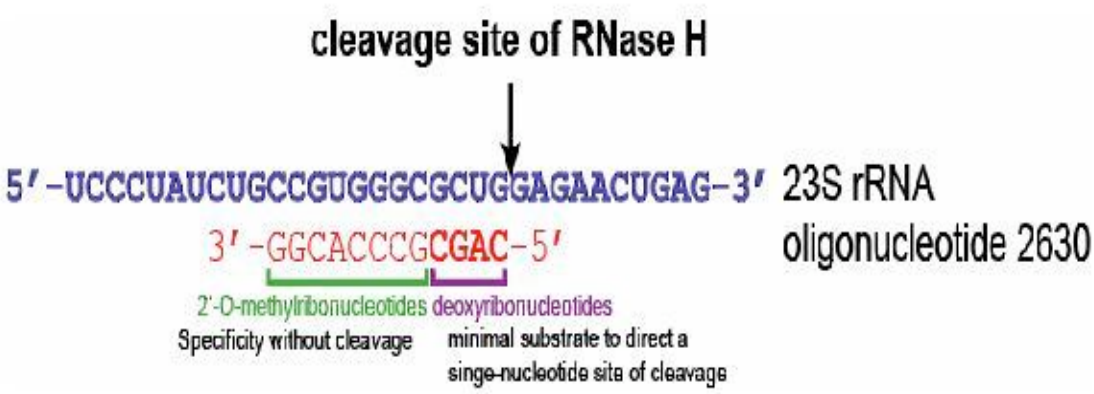

Figure 6. Chimeric oligonucleotide-directed cleavage of 23S rRNA by RNase H. Chimeric oligonucleotides were designed to contain four deoxynucleotides to direct the enzyme to a single-nucleotide site of cleavage, and eight 2'-*O*-methyl nucleotides to maintain a high level of specificity. Under these circumstances, the enzyme will cleave the RNA adjacent to the 5' end of the oligoneucleotide.

was scanned using a FLA-5000 phosphorimager. The radioactive and fluorescent bands were then analyzed to determine the approximate locations and specific radioactivities of tRNA crosslinks on the 23S rRNA.

For cleavage with chimeric oligonucleotides, the 10 μL reaction mix contained 0.2 A_{260} units of 23S rRNA, 1 μM of oligodeoxynucleotide 1612, and 1 μM of the selected chimeric oligonucleotide in Rnase H modifying buffer B. The reaction mix was incubated at 90 °C for 1 min, and then cooled to 55 °C by gradient heating over 8 min in a MiniCycler thermocycler (MJ Research). Without removing the tube from the thermocycler, the RNase H and RNasin, pre-diluted together in enzyme dilution buffer, were added to final concentrations of 0.25 U/μL and 1 U/μL respectively, and mixed by pipetting. The reaction mixture was then incubated, mixed with SYBR Gold and loading dye, and subjected to gel electrophoresis as described previously. The gel was scanned for SYBR Gold-fluorescent bands to verify that the reaction had gone to completion. The gel was then dried, covered with plastic wrap, and exposed to a phosphorimager screen. The screen was scanned using a FLA-5000 phosphorimager. The radioactive bands were then analyzed to determine the approximate locations and specific radioactivities of tRNA crosslinks on the 23S rRNA.

Precise localization of 23S rRNA crosslinks: The precise localization of tRNA-23S rRNA crosslinking sites was analyzed by primer extension. In this procedure, oligonucleotide primers were hybridized upstream of proposed crosslinking sites, and reverse transcriptase was used to extend a cDNA copy of the 23S rRNA until it approached a tRNA molecule covalently linked to the template. When the extension products were electrophoresed on a TBE sequencing gel, bands indicating extension

arrest were expected to occur one nucleotide upstream of the crosslinked site(s). The exact residue can be determined by comparing the mobility of the terminated fragment(s) to a 23S rRNA sequencing ladder run on the same gel. Because only a small percentage of the irradiated sample becomes crosslinked, the sample was first enriched for the crosslinked species by a preparative RNase H procedure.

RNase H digestion of 23S rRNA hybridized to oligonucleotides 1612 and 2368 (**Table 1**) permitted the isolation of fragments encompassing all presumed crosslinking sites (**Figure 7**). This procedure was executed following the method described above for RNase H cleavage using chimeric oligonucleotides. The reaction was scaled up proportionally to include 3 A_{260} units of 23S rRNA. When the digested samples were run on a gel, two SYBR Gold-dyed bands corresponding to the fragments 1612 – 2368 and 2369 – 3' end were produced. Two additional ^{32}P-labeled bands, detectible by autoradiography, were also expected. They were expected to have mobilities corresponding to the two stained/fluorescent fragments plus an additional 76 nucleotides attributable to crosslinked tRNA (**Figure 7**). These four bands were excised and placed into 1.5 mL microfuge tubes with 600 μL of RNA extraction buffer containing 0.01% Triton X-100. The fragments were eluted overnight on a rocking table.

The eluted rRNA was transferred to fresh tubes and was extracted three times with phenol/chloroform (1:1 mixture of phenol/chloroform in Na citrate, pH 4.7), and then two times with chloroform. 60 μL of Na acetate, pH 5.2 was added to each for a final concentration of 275 mM, and then they were each split equally into two microfuge tubes; 0.8 volume of isopropanol was added to each one and the 23S rRNA was precipitated on ice for 30 min, centrifuged for 60 min at 4 °C, rinsed with 200 μL of 70%

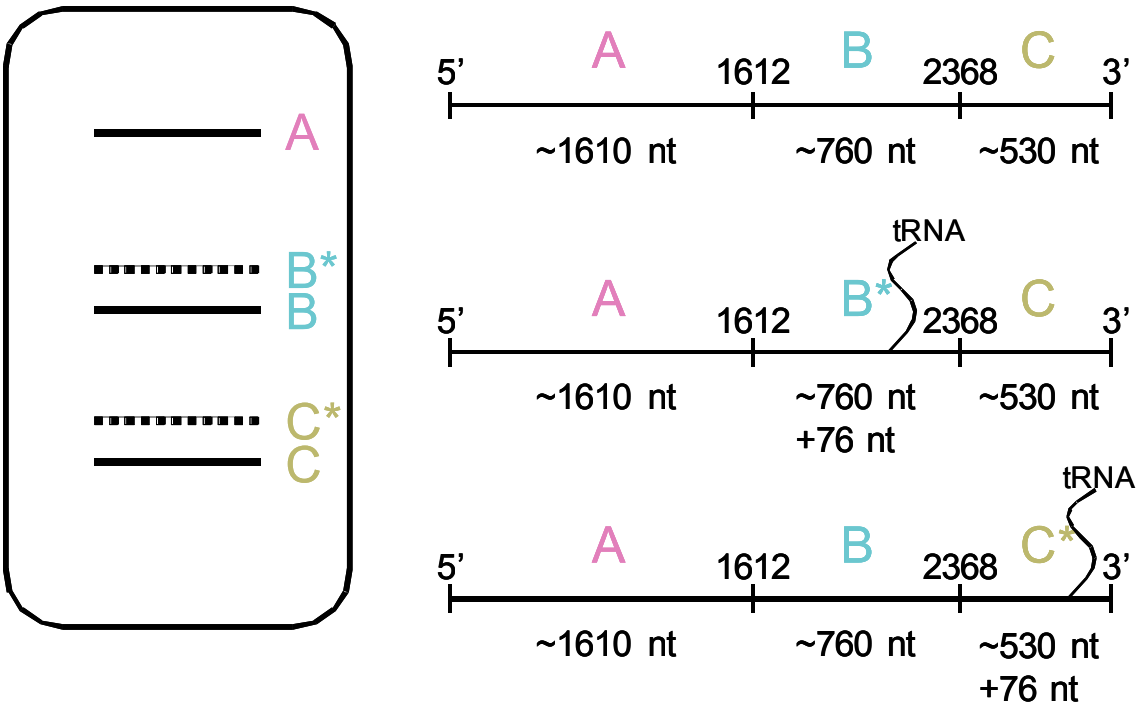

Figure 7. Isolation of primer extension templates by preparative RNase H digestion. To enrich for fragments crosslinked to tRNA, crosslinked 23S rRNA samples were digested with RNase H using oligoneucleotides 1612 and 2368. Because the samples contain a mixture of uncrosslinked 23S rRNA and 23S rRNA with tRNA covalently bound to one of multiple sites between neucleotide 1608 and the 3' end, the digestion produced five distinct fragments: **(A)** the 1610-nt uncrosslinked fragment from the 5' end of the 23S rRNA, **(B)** the 760-nt uncrosslinked fragment, **(B*)** the 760-nt fragment crosslinked to a 76-nt ^{32}P-labeled tRNA, **(C)** the 530-nt uncrosslinked fragment, and **(C*)** the 530-nt fragment crosslinked to a 76-nt ^{32}P-labeled tRNA. The uncrosslinked fragments (solid bands) were visualized on a 5% TTGP gel by SYBR gold staining. The crosslinked fragments (dashed bands) were not abundant enough to be visualized by SYBR gold, but were detectable by autoradiography. Bands B, B*, C, and C* were excised, extracted, and used as templates for primer extension analysis.

ethanol, and centrifuged again for 15 min. The supernatant was decanted and the 23S rRNA template was resuspended in 20 μL of 1X RNAsecure. Full-length crosslinked and uncrosslinked 23S rRNA controls were diluted to the approximate concentration of the RNase H-generated fragments.

In preparation for the primer extension procedure, primers 2667, 2579 and 2179 (**Table 1**) were labeled at their 5' ends with [γ-^{32}P]ATP in a 50 μL reaction containing 0.5 μM primer, 0.5 μM [γ-^{32}P]ATP, 10 U/mL yeast PPase, and 200 U/mL T4 PNK in kinase buffer. The reaction mix was incubated at 37 °C for 30 min, and the PNK was then inactivated by heating at 85 °C for two min. The labeled primers were cooled on ice before removing excess [γ-^{32}P]ATP by MicroSpin G-25 Sephadex columns.

The primers were hybridized individually to crosslinked and uncrosslinked fragments of the 23S rRNA, as well as the crosslinked and uncrosslinked full-length 23S rRNA. Primers 2667 and 2579 were used with fragments C and C*, and primer 2179 was used with fragments B and B* (**Figure 7**). All three primers were also used to scan the full-length 23S rRNA controls and for the generation of dideoxynucleotide sequencing ladders. In 0.5 mL microfuge tubes, each of the 10 μL reactions contained 6 μL of the diluted template and 1 μM labeled primer in hybridization buffer. Four additional hybridization reactions containing uncrosslinked 23S rRNA obtained from MRE600 ribosomes were prepared using each of the three primers in the same manner for generating dideoxynucleotide sequencing ladders. The primers were allowed to hybridize to the 23S rRNA by heating in a MiniCycler thermocycler (MJ Research) with a heated lid at 90 °C for one min, then reducing the heat to 65°C over 10 min by gradient cooling. The samples remained at 65°C for 5 min, and then were placed on ice for 2 min.

The tubes were centrifuged briefly to remove condensate from the cap and returned to ice until the primer extension reaction. The three sets of four sequencing-ladder templates were supplemented with 0.5 μL of either 1 mM ddC or 2.5 mM ddA, ddG, or ddT dideoxynucleotides. The ddC was used at a lower concentration because the frequency of incorporation was found to be too high relative to the other dideoxynucleotides and, as a result, less of the template sequence could be read.

AMV reverse transcriptase was used to extend the primers by mixing the 10- or 10.5-μL hybridization mixtures with 10 μL of extension mix composed of dNTPs, RNasin, AMV-RT and extension buffer to give a final reaction mixture containing primer-template hybrid with 320 μM dNTPs, 0.4 U/μL RNasin, and 0.4 U/μL AMV-RT in extension buffer. The tubes were mixed thoroughly by vortexing, and then spun briefly. The tubes were placed back in the thermocycler and incubated for 15 min at 42 °C with a heated lid. At the end of the incubation, the lid was removed and 120 μL of precipitation buffer was added to the warm samples and mixed by vortexing. The samples were immediately centrifuged at room temperature for 20 min at 14,000 rpm. After removing the supernatant, any remaining ethanol was allowed to evaporate by leaving the tubes open for 5-10 min. The pellets were dissolved in 15 μL of RNA loading dye and vortexed extensively to ensure complete resuspension. The samples were heated at 90 °C for 2 min and then 1.5 μL was loaded onto a pre-run 6% polyacrylamide sequencing gel with 0.5X TBE buffer in the upper tank and 1X TBE buffer in the lower tank. Na acetate was added to the lower tank to give a final concentration of 1 M after the sample entered the gel. The gel was electrophoresed at 55-65 W until the bromophenol blue reached the bottom. After electrophoresis, the gel was

removed from the plates, dried, covered with plastic wrap, and exposed to a phosphorimager screen. The screen was scanned using a FLA-5000 phosphorimager. The radioactive bands indicating reverse transcriptase stop sites were then compared to the sequencing lanes to determine the precise locations of the crosslinked nucleotides.

CHAPTER 3

RESULTS

Growth of Bacterial Strains

E. coli BL21(DE3) cells carrying pGST-MS2, which encodes the GST-MS2 fusion protein for use in the isolation of MS2-tagged ribosomes under *lac* control, were grown on LB agar plates with ampicillin at 37 °C. Many large colonies were produced after an incubation period of about 20 hr. Liquid LB medium was inoculated with a single colony and cells were grown at 37 °C until the OD_{600} reached 0.5-0.6 with a doubling time of 28 min **(Table 2)**. Protein expression was induced by the addition of IPTG at room temperature. After incubation for 2 hr with IPTG, GST-MS2 was detected when the cells were lysed and their contents analyzed by SDS-PAGE. A relatively large increase in the level of GST-MS2 was detected 21 hr post-induction **(Figure 8A)**.

Plasmid p278MS2 encodes the gene for 23S rRNA with an MS2 affinity-tag inserted at the terminal loop of helix 98 under control of the lambda repressor. Mutations in the 23S rRNA gene were made at positions A2451, U2506, U2585, and A2602 (Youngman et al., 2004). *E. coli* DH10 pcI857 cells containing p278MS2, p278MS2(U2506G), and p278MS2(U2585A) were grown at 30 °C on LB agar plates and then in liquid LB medium at 42 °C to induce synthesis of the mutant 23S rRNA by inactivation of the temperature-sensitive lambda repressor carried on pcI857. Both the solid and liquid media contained ampicillin and kanamycin. After approximately 24 hr of incubation on LB agar plates, the three strains produced many very small colonies. In 42 °C liquid medium, the strains, p278MS2, p278MS2(U2506G), and p278MS2(U2585A), grew with similar doubling times of 29 min, 27 min, and 30 min, respectively **(Table 2)**.

Table 2. Strain doubling times

Strain	Doubling Time (min)
BL21(DE3) pGST-MS2	28
DH10 p278MS2	29
DH10 p278MS2(U2585A)	30
DH10 p278MS2(U2506G)	27

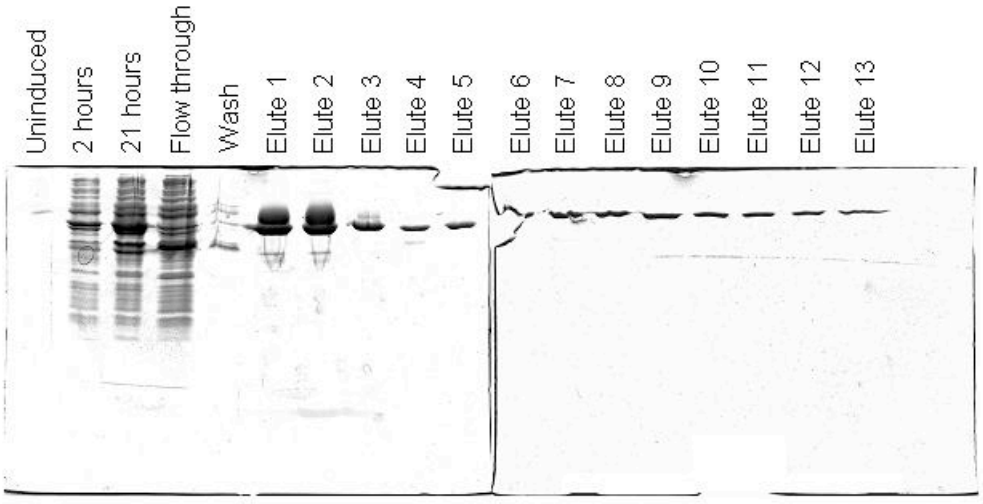

A

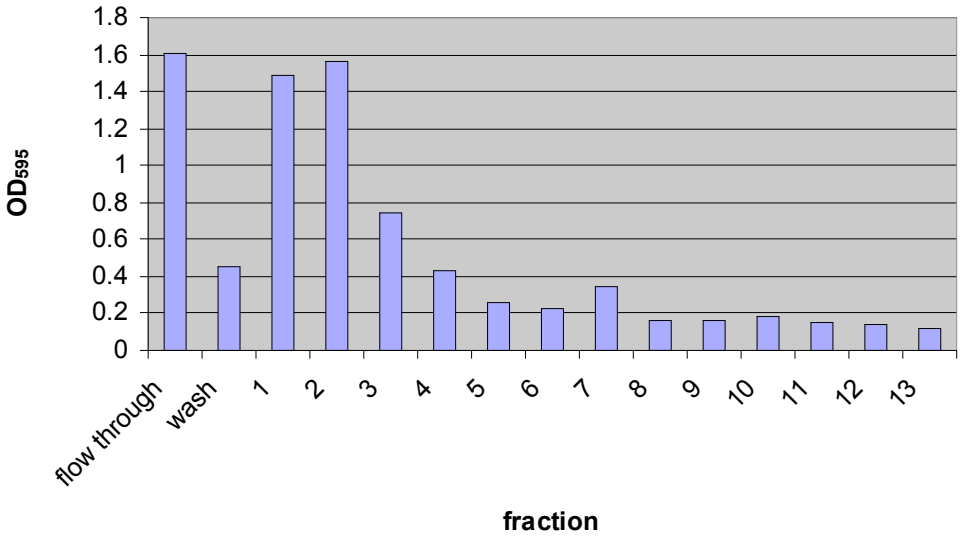

B

Figure 8. Expression of GST-MS2 fusion protein. **(A)** 12% SDS-PAGE of GST-MS2 expression and GS-column fractions. Lanes 1-3 represent crude protein from BL21(DE3) pGST-MS2 cells prior to induction, 2 hours post-induction, and 21 hours post-induction. Lanes 4-18 represent flow-through, wash, and elution fractions from GST-MS2 purification on a GS-column. **(B)** Relative concentration of protein in GS-column fractions. Each measurement represents the absorbance at 595 nm of 20-µL samples of each fraction in 1 mL of Bio-Rad protein assay solution.

Ribosome Preparation

A glutathione sepharose (GS) column was used to purify the GST-MS2 fusion protein from the cell lysate **(Figure 8B)**. Samples of each fraction were checked by SDS-PAGE **(Figure 8A)**. BSA was used as a standard to determine the concentration of protein by the Bio-Rad protein (Bradford) assay. The amount of protein collected was inconsistent. The yield varied from 3.0 mg to 11.7 mg of protein per L of growth medium from cell preparations of similar cell densities ($OD_{600} \approx 0.5$). The poor yield from some preparations may have been due to poor column regeneration.

Crude 70S ribosomes were prepared from DH10 p278MS2 cells and the two strains carrying 23S rRNA mutations. The MS2-tagged ribosomes were separated from DH10 wild-type ribosomes by passing them through a GSTrap affinity column preloaded with GST-MS2 fusion protein **(Figure 9)**. The expected recovery of MS2-tagged ribosomes is 5-10% of the total amount of ribosomes in the crude lysate (Youngman et al., 2004). In the present experiments, the typical recovery was 3-5% prior to concentration in an Amicon Ultra centrifugal filter device. During concentration approximately half of the recovered ribosomes were lost, possibly from sticking to the filter, resulting in 1-3% final recovery. There was no improvement in the ribosome yield after implementing the modifications described in Materials and Methods.

To confirm the presence of the MS2 tag in the eluted ribosomes, RNase H analysis was used. Wild-type 23S rRNA should yield a digestion product of 114-129 nt from the 3' end when digested with RNase H in the presence of oligonucleotide #1. Mutant rRNA containing the 32-nt insert should yield a 146-161 nt 3'-end product under the same circumstances. The analysis of the digestion products revealed that there is a

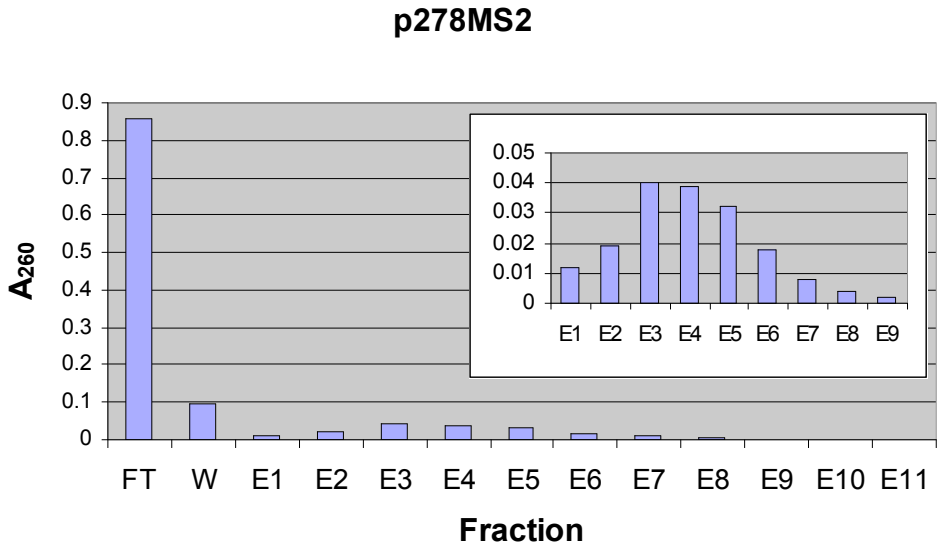

A

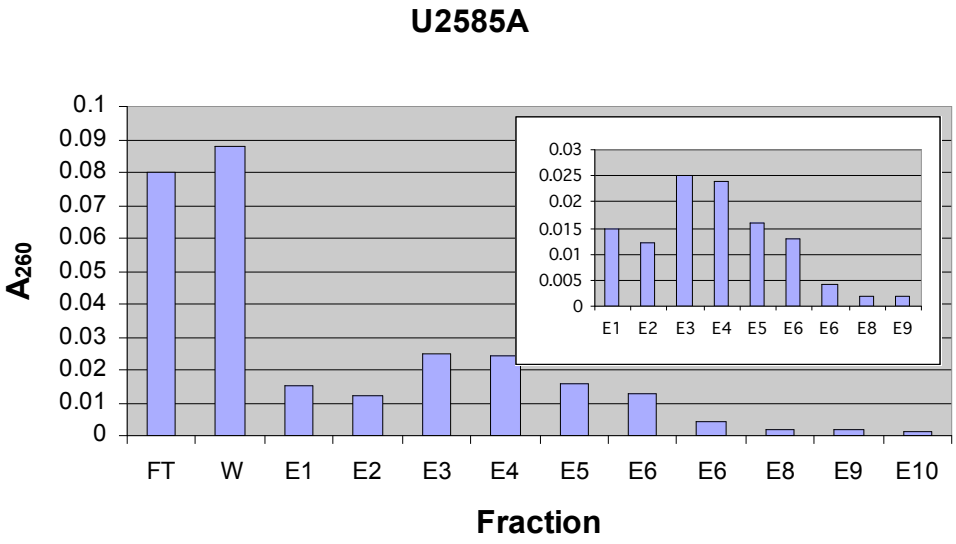

B

Figure 9. Purification of MS2-tagged ribosomes on GSTrap affinity columns. **A**, **B**, and **C** show the relative concentrations of p278MS2, p278MS2(U2585A), and p278MS2(U2506G) 70S ribosomes in column fractions. Each measurement represents the absorbance at 260 nm of 5-µL samples of each fraction diluted in 1 mL of water. Insets show elution data on an expanded scale.

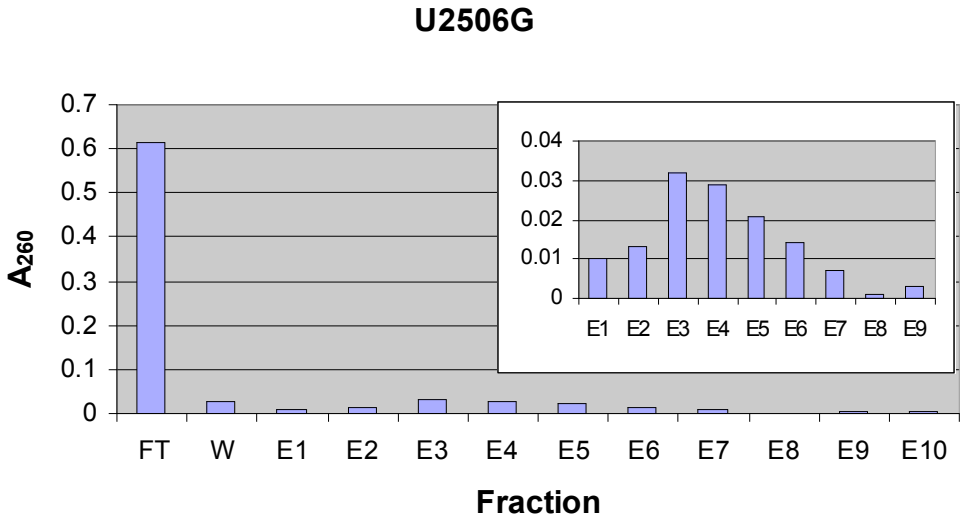
U2506G
0.7
0.6
0.5
0.4
0.3
0.2
0.1
0
A260
FT
W
E1
E2
E3
E4
E5
E6
E7
E8
E9
E10
Fraction
0.04
0.03
0.02
0.01
0
E1
E2
E3
E4
E5
E6
E7
E8
E9

C

difference between the mobility of the fragment produced by tagged 23S rRNA and that of wild-type 23S rRNA **(Figure 10)**. This evidence suggests that the 32-nucleotide insert is present in the eluted p278MS2 ribosomes.

Preparation of ^{32}P-labeled [2N_3A76]tRNA^{Phe}

The photoreactive substrate, ^{32}P-labeled (2N_3A76)tRNA^{Phe}, was prepared by first labeling the 5' position of 2-azidoadenosine bisphosphate (p2N_3Ap) with [γ-^{32}P]ATP. The labeling reaction, catalyzed by PNK, was 60-77% efficient, labeling 3-4% of the p2N_3Ap **(Figure 11)**. Using T4 RNA ligase, [5'-^{32}P]p2N_3Ap was then ligated to the 3' end of tRNA^{Phe} lacking the 3'-terminal A76. 13-24% of the total tRNA was ligated to 23-43% of the labeled bisphosphate. This calculation was based on the amount of radioactivity transferred from the [5'-^{32}P]p2N_3Ap to tRNA, and it does not take into account the tRNA that was lost during the purification procedures.

Binding and Crosslinking

^{32}P-labeled (2N_3A76)tRNA^{Phe} was bound and crosslinked to 70S ribosomes from MRE600, and from DH10 expressing 23S rRNA from p278MS2, p278MS2(U2506G), and p278MS2(U2585A) to analyze how the 3' end of tRNA interacts with the P-site of wild-type and mutant ribosomes. Binding and crosslinking procedures were performed for several experiments. The data are presented in **Table 3**.

A nitrocellulose filter assay was used to evaluate the efficiency of binding and crosslinking of ^{32}P-labeled (2N_3A76)tRNA^{Phe} to the wild-type and mutant ribosomes. The tRNA was bound to the P-site of 70S ribosomes in the presence of poly (U), and samples were passed through a nitrocellulose filter, which traps tRNA-ribosome

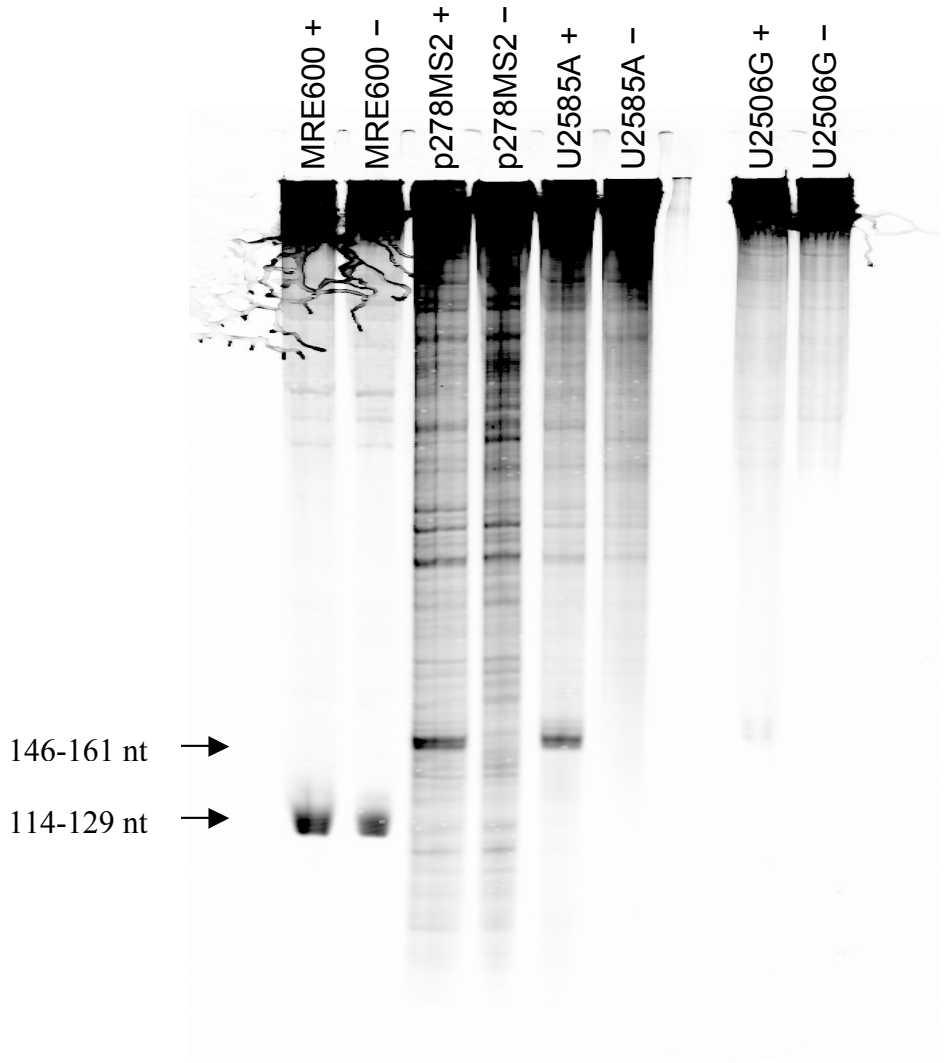

Figure 10. Verification of purity of MS2-tagged ribosomes. 5% TTGP gel of RNase H digestion fragments (+ oligonucleotide) and oligonucleotide control digests (− oligonucleotide) confirming the presence of the MS2 insert in mutant ribosomes. Tagged 23S rRNA digested with RNase H in the presence of oligonucleotide #1 yields a 146-161 nt 3' fragment, whereas untagged MRE600 23S rRNA yields a 114-129 nt 3' fragment. (There is a faint band present in the "U2506G +" lane.) Because the wild-type MRE600 23S rRNA was not purified by the Nucleobond AX procedure, 5S rRNA is present in the MRE600 digests. Due to the presence of 5S rRNA, the band corresponding to the 3' fragment in the MRE600 lane is difficult to detect. This is because MRE600 5S rRNA is 120 nucleotides long (Szymanski et al., 2002), which is approximately the same length as the expected RNase-derived fragment (114-129 nt). A control reaction of the MRE600 rRNA, in which oligonucleotide #1 was not added ("MRE600 −"), reveals the band corresponding to 5S rRNA. Since the band in the test lane appears more intense than the band in the control lane, it is likely that the former represents both the 5S rRNA and the 3' fragment.

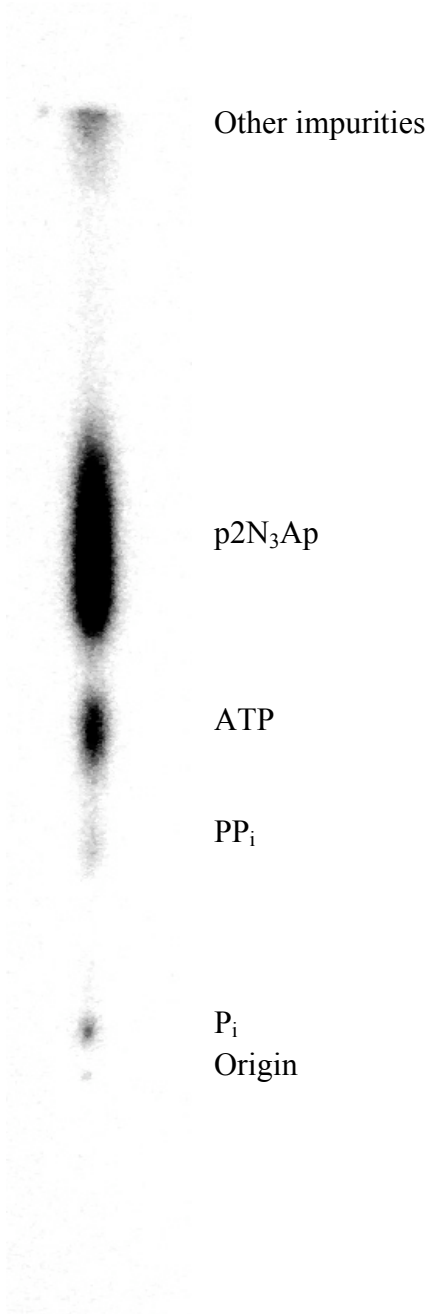

Figure 11. Labeling of $p2N_3Ap$ with ^{32}P. An autoradiographic image of [5'-^{32}P]$p2N_3Ap$ after labeling with [γ-^{32}P]ATP. The reaction mixture was separated by cellulose PEI-TLC using 0.75 M KH_2PO_4, pH 3.5 as a running buffer. 3.6% of the $p2N_3Ap$ was labeled by 72% of the total [γ-^{32}P]ATP.

Table 3. Binding and crosslinking of [2N$_3$A76]tRNA^{Phe} to wild-type and mutant ribosomes

Strain	Percent of total tRNA noncovalently bound to 70S ribosomes[a]							Percent of total tRNA crosslinked to 50S subunit[b]							Percent of covalently bound tRNA crosslinked to 50S subunit[c]						
	A[d]	B	C	D	E	F	G	A	B	C	D	E	F	G	A	B	C	D	E	F	G
MRE600	22	20	11	15	4	35	52	22	6	3	4	3	4	4	102	28	27	26	87	12	8
p278MS2	13	17	7	21	5	30	40	4	6	2	5	3	4	5	27	34	34	25	66	12	12
p278MS2 (U2585A)	14	17	12	24	7			4	5	2	5	3			26	26	18	21	44		
p278MS2 (U2506G)	15	11	7	23	8	40	46	6	4	1	6	4	4	6	40	32	10	26	52	11	14

a. Radioactivity of noncovalently bound tRNA on filter/ total radioactivity applied to filter
b. Radioactivity of covalently bound tRNA on filter/ total radioactivity applied to filter
c. (b.) / (a.)
d. A-G represent individual binding and crosslinking trials. Experiments F and G do not include U2585A due to the limited availability of material.

complexes, while allowing free tRNA to pass through. The amount of radioactivity retained on the filter was measured by scintillation counting and compared to the total radioactivity applied to the filter to determine the percentage of tRNA non-covalently bound to the 70S ribosomes.

The non-covalent complexes were irradiated with UV light at 300 nm to covalently crosslink the photoreactive tRNA to the P-site of the ribosomes. A similar filter-binding assay was performed to determine the percentage of total tRNA that was crosslinked to the ribosomes. In this assay, the samples were diluted into a low-magnesium buffer to dissociate the 50S and 30S subunits, releasing any non-covalently bound tRNA. The percentage of total tRNA that was crosslinked to the ribosomes was calculated. The percentage of non-covalently bound tRNA that became crosslinked was also calculated.

The binding and crosslinking data for each type of ribosome vary greatly between the experiments presented in **Table 3**. However, in several experiments, the data show similarities between the wild-type and mutant ribosomes, with only a few anomalies. Also, more recent trials (F and G) show increased binding efficiency due to improvements in experimental technique. There is no discernable pattern in the differences observed between wild-type and mutant ribosomes, suggesting that the point mutations U2506G and U2585A in 23S rRNA do not interfere with tRNA binding and crosslinking to the P-site.

Collection of tRNA-ribosome complexes

For the analysis of tRNA-ribosome crosslinking patterns, 50S subunits, 23S rRNA, and 50S-subunit proteins were isolated. To collect the 23S rRNA and ribosomal

proteins, crosslinked 70S ribosomes were dissociated in urea and passed through a Nucleobond AX 20 ion-exchange column. The flow-through, which contained crosslinked proteins and free ^{32}P-labelled tRNA, was collected and used for later analysis of tRNA-protein crosslinks following S1 digestion. 23S rRNA was retained on the column and eluted with NaCl. Based on measurements by a scintillation counter **(Figure 12)**, fractions containing 23S rRNA were pooled for use in RNase H and primer extension analyses. The 23S rRNA fractions corresponded to 1.6-2.5% of the total radioactivity loaded onto the column.

In some experiments, 50S subunits were first separated from crosslinked 70S ribosomes on 15-30% sucrose gradients. The gradient buffer contained a low magnesium concentration to dissociate the 50S and 30S subunits. Using the UV and radioactivity profiles **(Figure 13)**, fractions containing 50S subunits were pooled and prepared for use in subsequent analyses.

An interesting phenomenon observed in the UV profiles of the mutant ribosomes is the presence of an unknown "40S" product that migrates between the 30S and 50S subunits. In some experiments, the product is also visible as a relatively minor peak in the profile of non-mutated p278MS2 ribosomes that contain the MS2 insert. MRE600 ribosomes show no signs of the "40S" peak. It is possible that this peak corresponds to a precursor 50S subunit containing 23S rRNA with the MS2 insert, which may slow the rate of 50S assembly. It is also possible that the peak represents a malformed 50S subunit, although there is no abnormal growth phenotype exhibited by cells expressing 23S rRNA from p278MS2 (Youngman et al., 2004). Another potential cause of this anomaly may be some adverse effect due to the affinity chromatography method used in

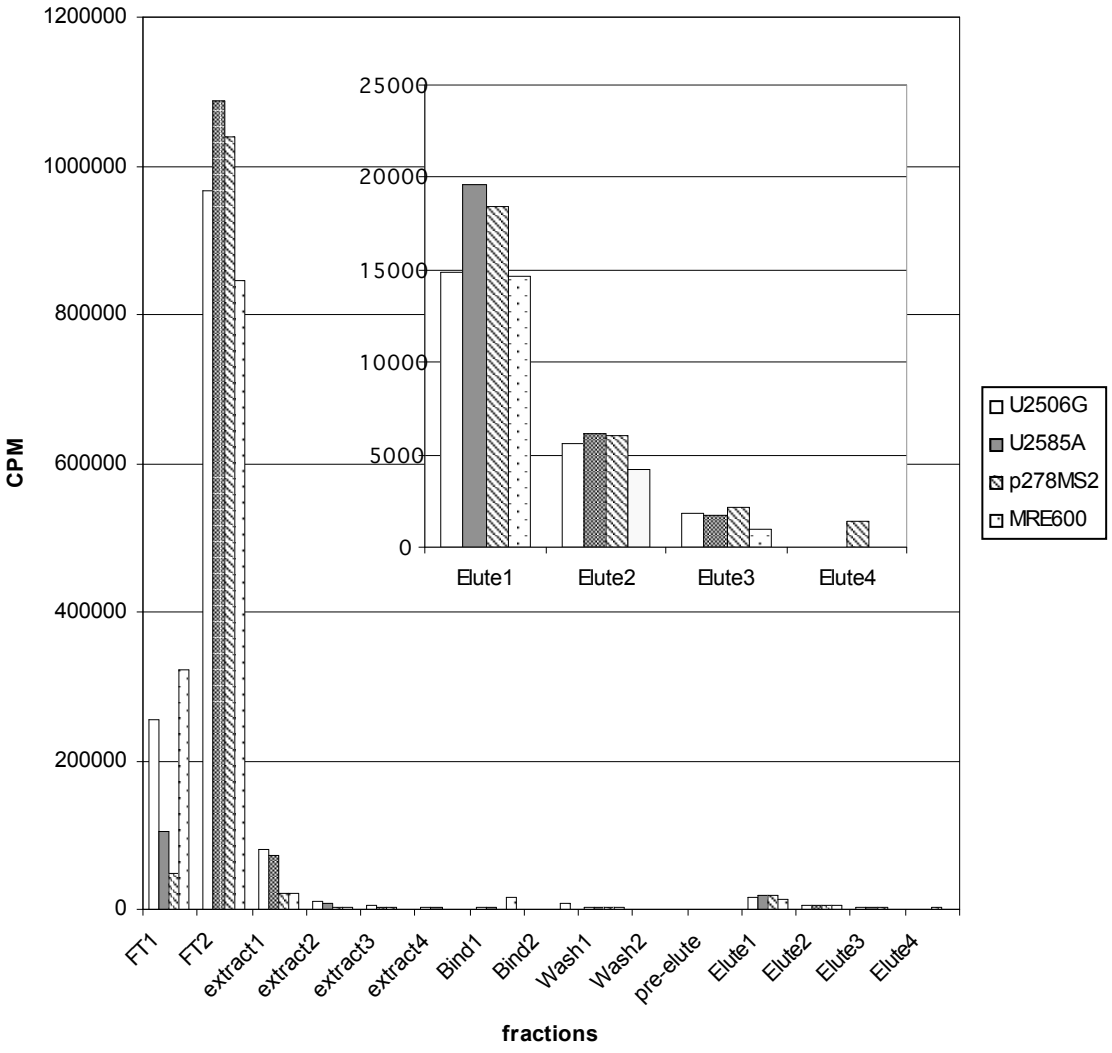

Figure 12. Profile of radioactive material found in Nucleobond AX column fractions. Crosslinked 23S rRNA and ribosomal proteins were separated by a Nucleobond AX column. The flow-through (FT), containing crosslinked proteins and free ^{32}P-labelled tRNA, and elution fractions 1-4, containing 23S rRNA, were collected for analysis by gel electrophoresis. Inset shows 23S rRNA elution pattern on an expanded scale.

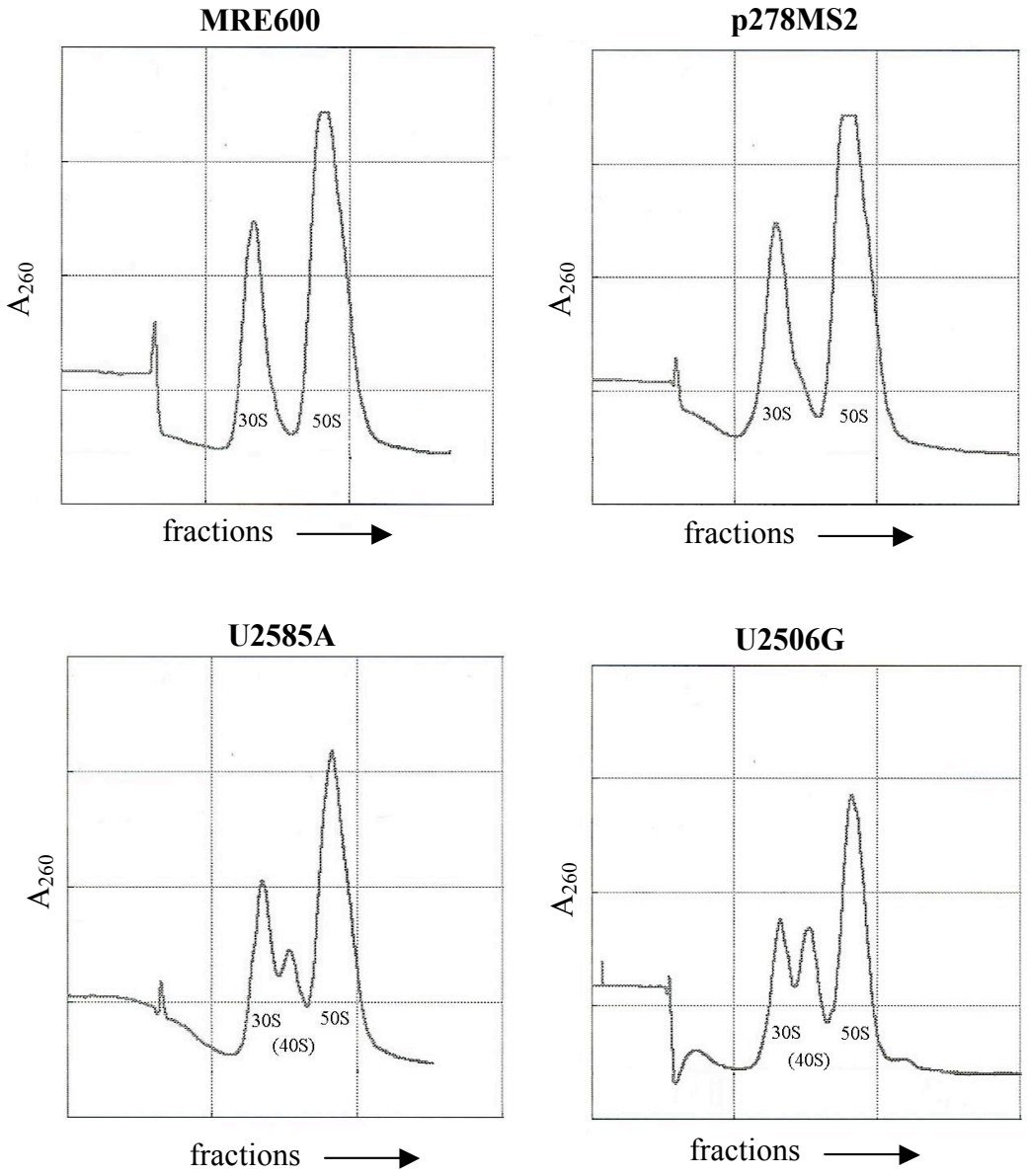

A

Figure 13. Fractionation of crosslinked ribosomal complexes by sucrose-gradient fractionation. The crosslinked 70S ribosomes were separated on 15-30% sucrose gradients and the fractions containing 50S subunits were collected. **(A)** UV profile; **(B)** ^{32}P radioactivity profile.

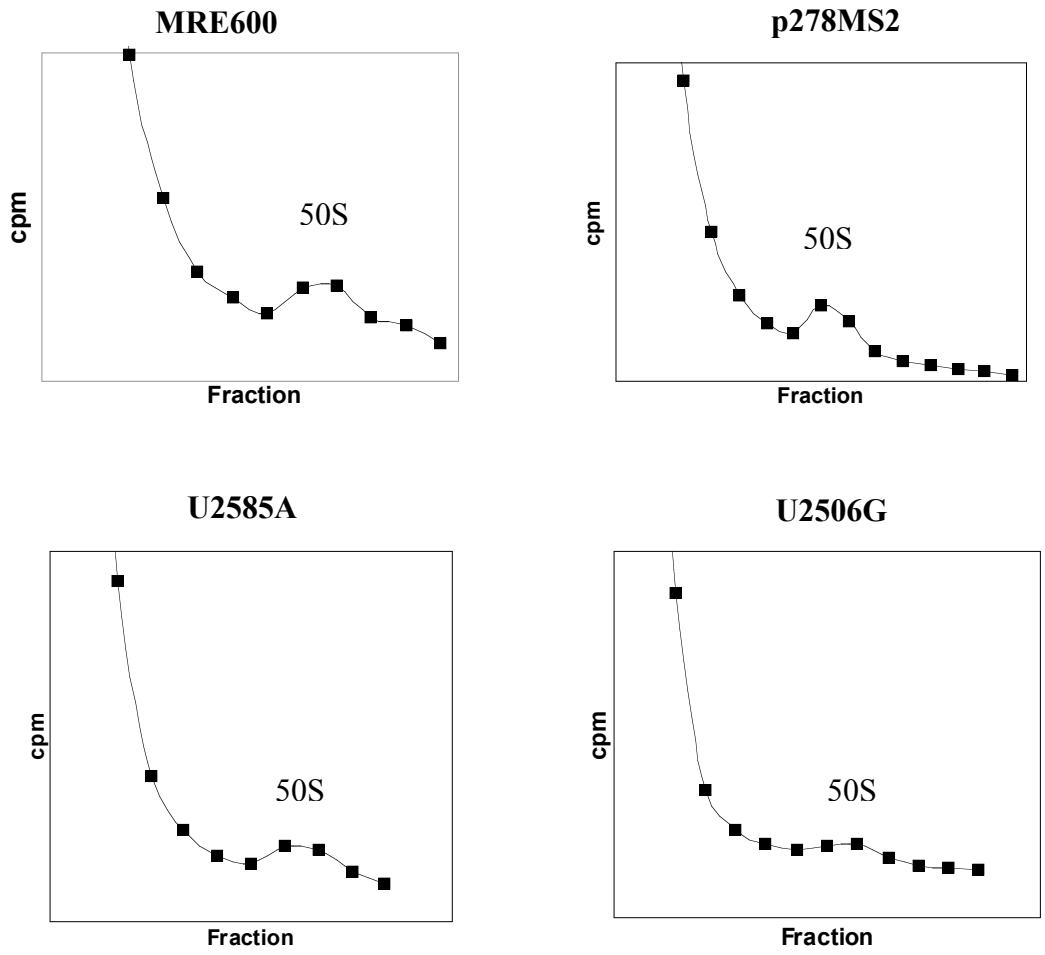

B

the isolation of the tagged ribosomes, although the Zimmermann lab has ruled out any effect on cell growth at 42 °C *per se* (J. Robin, personal communication). A more interesting cause of this "40S" peak would be any structural changes due to the point mutations at nucleotides U2585 and U2506.

Analysis of tRNA-ribosome complexes

The 50S subunits collected by sucrose gradient fractionation were used to determine the distribution of tRNA crosslinks between the 23S rRNA and 50S-subunit proteins. Analyses for most experiments were inconclusive owing to variability in the results. One initial set of results showed that the distribution of crosslinks between 23S rRNA and ribosomal proteins is similar in complexes from the U2585A mutant ribosomes and from p278MS2 and MRE600 wild-type ribosomes **(Figure 14)**. For these ribosomes, 51-54% of the crosslinked ligand were bound to 23S rRNA and 46-49% were bound to protein. The distribution was shifted in the U2506G mutant where 66% were bound to 23S rRNA and 34% were bound to protein. The data from this experiment suggest that nucleotide U2506 may affect the positioning of the 3' end of tRNA relative to the ribosomal proteins. However, no other trials have supported these data, and some results have even shown that triplicates of the same sample that are run on the same gel will appear quantitatively different.

Analysis of tRNA-protein complexes

Crosslinked protein-tRNA complexes, collected from the 50S fractions of sucrose gradients or from the Nucleobond AX-column flow-through fractions, were digested with S1 nuclease to determine the distribution of crosslinks between 50S-subunit proteins L27 and L33. S1 nuclease digests all RNA nonspecifically. Because it cleaves the tRNA to

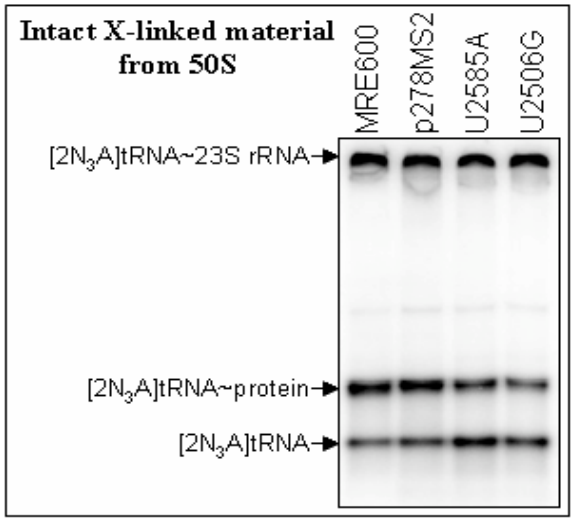

A

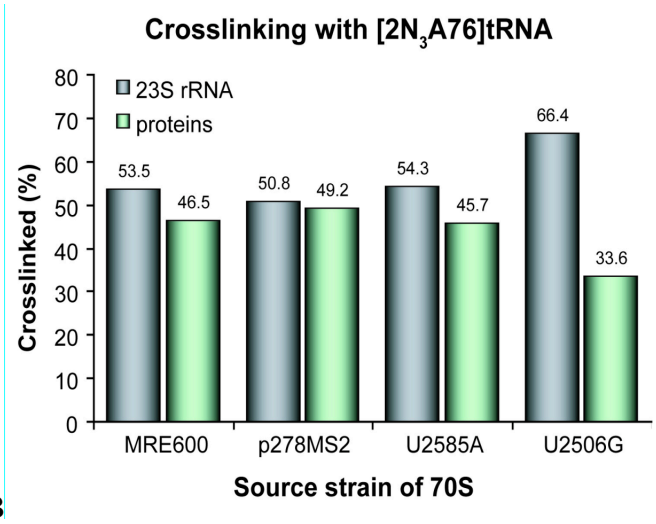

B

Figure 14. Distribution of crosslinks between 23S rRNA and 50S-subunit proteins. **A)** Intact crosslinked material from 50S subunits was resolved by 4-20% SDS-PAGE. **B)** For crosslinked ribosomes prepared in experiment B (Table 3), the distribution of crosslinks between 23S rRNA and ribosomal proteins is similar in complexes from the MRE600, p278MS2, and U2585A ribosomes (51-54% tRNA-23S rRNA: 46-49% protein), whereas the distribution is shifted in the complexes from the U2506G ribosomes (66% 23S rRNA: 33% proteins).

produce 3'OH and 5'P, S1 nuclease leaves the proteins covalently linked to [5'-^{32}P]AMP from the 3' end of the tRNA. Two bands corresponding to L27 and L33 are expected to be visualized by SDS-PAGE analysis of the products from the S1 nuclease digestion; L27 is present at the PTC where it may contribute to peptide bond formation (Maguire et al., 2005), while L33 is located at the E site and becomes crosslinked to the small amount of P-site tRNA that spills into the E site (Wower et al, 1994).

In the present experiments, only one band was present on the gels from the digests of wild-type and mutant ribosomes. One possibility may be that the gels required a longer running time to resolve the two bands, which migrate at a similar rate. Additionally, the samples obtained from the Nucleobond AX column flow-through contained crosslinked proteins, free ^{32}P-labelled tRNA, and free ^{32}P nucleotides. These may have interfered with the analysis because more than 90% of the total radioactivity loaded on the column was found in the flow-through. In future experiments it would be preferable to digest the sample with S1 nuclease prior to concentration in a centrifugal filter device in order to reduce the radioactive material from free ^{32}P-labelled tRNA as much as possible. Since S1 nuclease digests all RNA, the abundance of free, radioactive tRNA would be degraded to single nucleotides, which would readily pass through the filter.

Analysis of tRNA-23S rRNA complexes

Partial localization of 23S rRNA crosslinks: A major goal of these experiments was to determine the locations of the tRNA crosslinks on the 23S rRNA. To obtain an approximate localization, the tRNA-23S rRNA complexes obtained by Nucleobond AX columns were cleaved into specific segments using RNase H, an enzyme that degrades

the RNA in an RNA:DNA duplex. A series of oligodeoxyribonucleotides complementary to specific sequences in 23S rRNA were utilized for this purpose **(Table 1, Figure 15)**. RNase H digestion of the 23S rRNA using two oligonucleotides (ex. a and b) produces three rRNA fragments (5' end- oligonucleotide a; oligonucleotide a – oligonucleotide b; oligonucleotide b – 3' end) that can be resolved on a 5% polyacrylamide gel. If the fragments contain a site of crosslinking of ^{32}P-labeled $(2N_3A76)tRNA^{Phe}$, the corresponding band will be detectable by autoradiography.

A series of digestion products from each tRNA-23S rRNA complex was analyzed under non-denaturing conditions on a polyacrylamide gel. Gel bands were imaged using both SYBR Gold staining and radioactivity **(Figure 16A)**. For each fragment, quantitative data from the SYBR Gold-fluorescent bands was used to determine the mass of the fragment and the ratio of radioactivity to mass was determined. The information from the overlapping fragments was used to deduce the percentage of tRNA crosslinked to the various segments of the 23S rRNA **(Figure 16B)**.

The RNase H digestion results are shown for p278MS2, U2585A, and U2506G. Because the radioactivity level was low for the MRE600 sample, the wild-type results shown are from previous experiments in the Zimmermann lab. Wower et al. (2000) previously showed that P-site-bound $(2N_3A76)tRNA^{Phe}$ forms crosslinks to nucleotides U2585 and U2506. The results for MRE600 are consistent with these observations as shown in figure 16B, where a large percentage of the radioactivity appears to be in the fragments from oligonucleotides 4 to 3b and from 3 to 2a, which contain nucleotides U2506 and U2585, respectively. Although the error for all of the calculations is high, the data from the digests of the

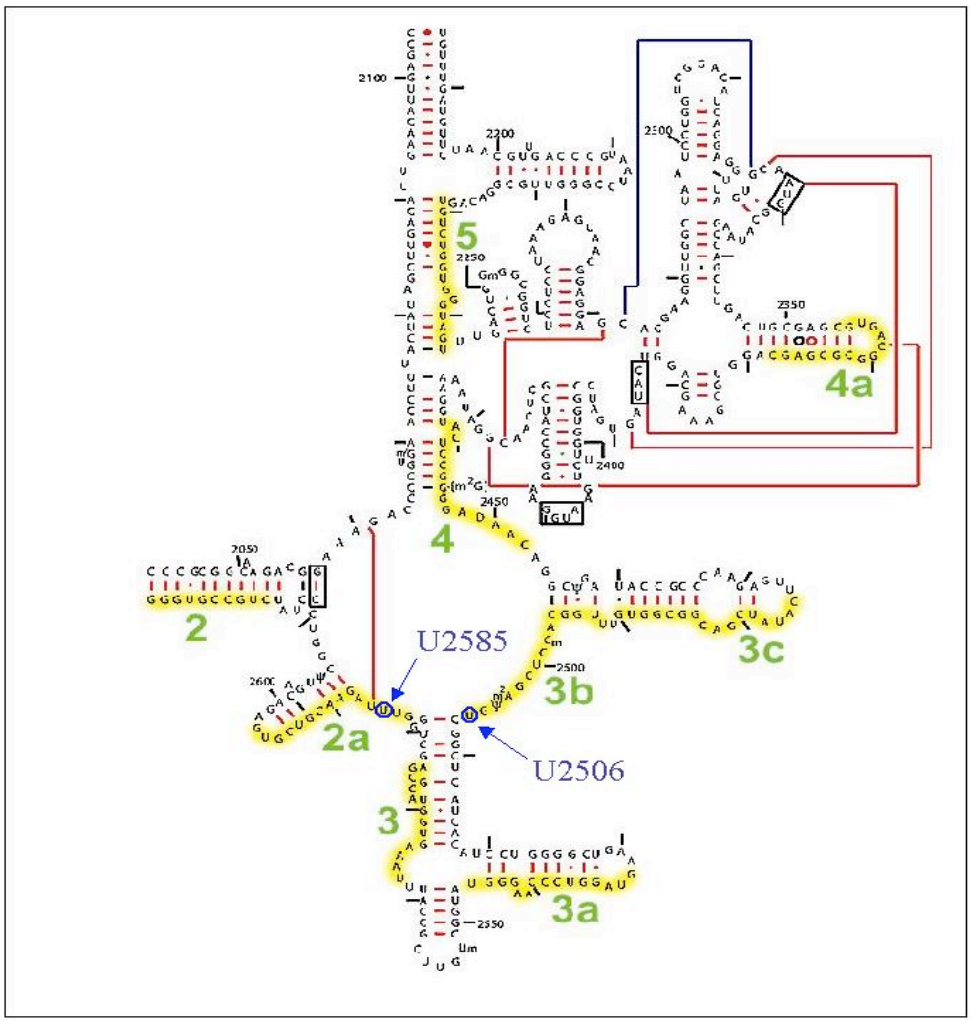

Figure 15. Sequences to which oligonucleotides hybridize on 23S rRNA. The yellow highlighted regions represent the sites where oligonucleotide primers (Table 1), used for RNase H analysis, hybridize to domain V of the 23S rRNA. Wower et al. (2000) previously showed that P site-bound [$2N_3$A76]tRNA^{Phe} forms crosslinks to nucleotides U2585 and U2506 (circled in blue).

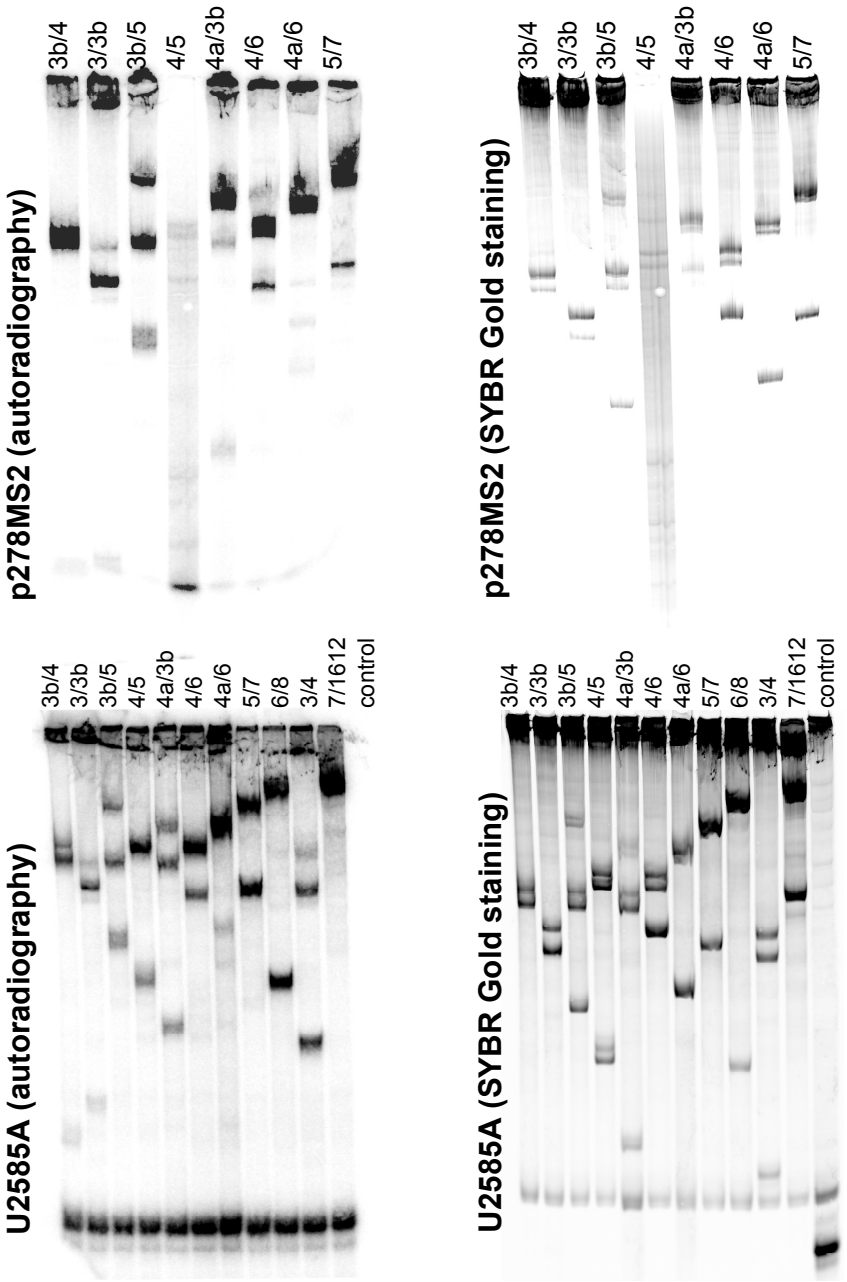

Figure 16. Analysis of tRNA-23S rRNA complexes by RNase H digestion. **(A)** 5% TTGP gels of RNase H-digestion products. For each fragment whose boundaries are indicated by the oligonucleotide numbers above the lanes, quantitative data from the SYBR Gold-fluorescent bands was used to determine the mass of the fragment and the ratio of radioactivity to mass was determined. **(B)** Percentage of tRNA crosslinking to each region of 23S rRNA. (MRE600 data were from an experiment by A. Manuilov.) Information from the overlapping fragments was used to deduce the percentage of tRNA crosslinked to the various segments of the 23S rRNA. The large percentage of radioactivity in the fragments from oligonucleotides 4 to 3b and from 3 to 2a in the MRE600 analysis suggests that there are tRNA crosslinks at positions U2585 and U2506 as proposed by Wower et al. (2000). Similarly, the data from the digests of p278MS2, U2585A, and U2506G ribosomes suggest that there is a crosslink in the vicinity of U2585; however, the information regarding a possible U2506 crosslink is inconclusive.

A

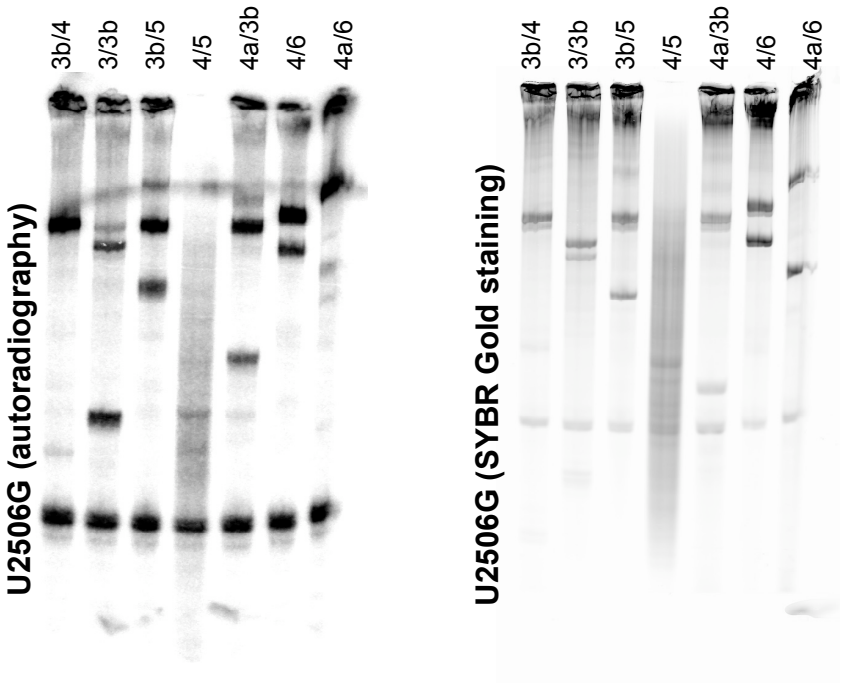
3b/4
3/3b
3b/5
4/5
4a/3b
4/6
4a/6
U2506G (autoradiography)
3b/4
3/3b
3b/5
4/5
4a/3b
4/6
4a/6
U2506G (SYBR Gold staining)

B

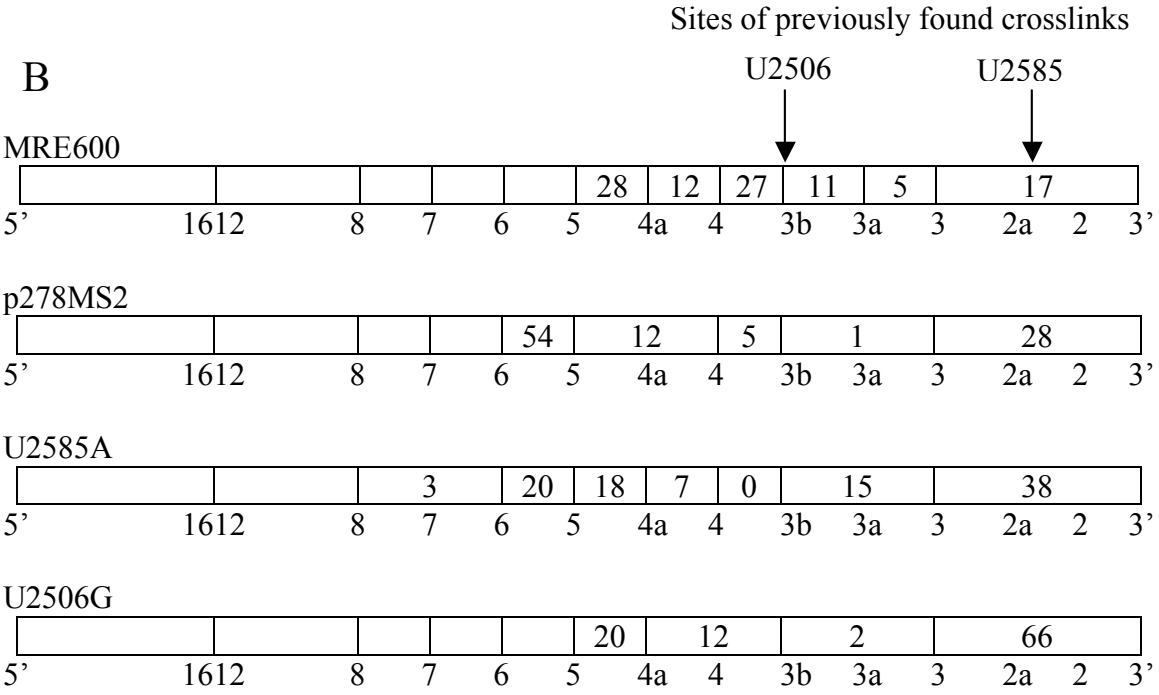
Sites of previously found crosslinks
U2506
U2585
MRE600
28 12 27 11 5 17
p278MS2
54 12 5 1 28
U2585A
3 20 18 7 0 15 38
U2506G
20 12 2 66
5’ 16 12 8 7 6 5 4a 4 3b 3a 3 2a 2 3’

tagged wild-type and mutant ribosomes suggest that there is a crosslink in the vicinity of U2585, because of the high level of radioactivity in the fragment from the position of oligonucleotide 3 to the 3' end. Further RNaseH digestion in the vicinity of U2506 is required to localize the radioactivity to a smaller segment of the 23S rRNA.

There are several aspects of this method that hinder the accuracy of the localization and quantification of crosslinking along the 23S rRNA. Unfortunately, oligonucleotides 2a and 3b overlap the two primary sites of interest, U2585 and U2506, respectively. Although RNase H tends to cut the RNA near the 5' end of the oligodeoxynucleotide, the precise site(s) of digestion is difficult to predict. Therefore, the crosslink could potentially be on either side of the cleavage site. Also, the bulky tRNA covalently bound to these positions may impede oligonucleotide hybridization or RNase H digestion, resulting in inaccurate quantification. Another drawback to these experiments is that the native gel conditions used for the fractionation of the RNase H digests may prevent some of the products from dissociating due to secondary-structure interactions.

Because of these problems, most of the oligonucleotide primers were redesigned as chimeric oligonucleotides containing blocks of deoxynucleotides and 2'-*O*-methyl nucleotides to increase the specificity of the analysis **(Table 1, Figures 6 and 17)**. Because RNase H will specifically cut the RNA adjacent to the 5' end of such chimeric oligonucleotides, the cleavage sites are unambiguous, allowing for more accurate quantification. The chimeric oligonucleotides were also designed to bracket the proposed sites of crosslinking to avoid problems with hybridization. Results obtained using the chimeric oligonucleotides have shown that crosslinks are likely to occur in the vicinity of

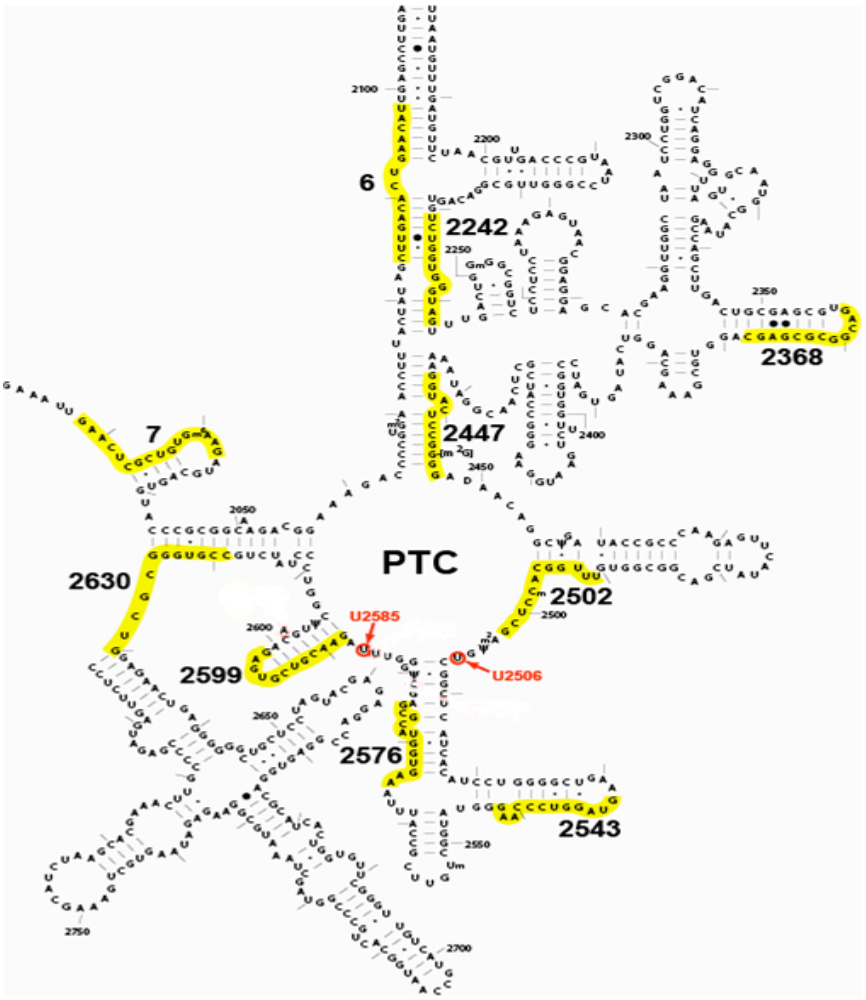

Figure 17. Sequence to which chimeric oligonucleotides hybridize on 23S rRNA. The yellow highlighted regions represent the sites where oligonucleotide primers (Table 1), used for RNase H analysis, hybridize to domain V of the 23S rRNA. Wower et al. (2000) previously showed that P site-bound [$2N_3$A76]tRNA^{Phe} forms crosslinks to nucleotides U2585 and U2506 (circled in red).

nucleotides 2585 and 2506, because of the high level of radioactivity that is present between oligonucleotides 2502 and 2576, and between 2576 and 2599 **(Figures 18 and 19)**. Additionally, the preliminary data suggest that, in the U2506G mutant, the ligand may crosslink preferentially to nucleotide U2506G relative to other crosslinking sites. In the two samples without point mutations, MRE600 and p278MS2, approximately 20-30% of the crosslinking occurs in the segment containing U2585, and another 30% of the crosslinking occurs in the region containing U2506. Only 14-15% of the crosslinking in the U2585A and U2506G samples occurs in the U2585 region of the 23S rRNA. However, tRNA appears to preferentially crosslink to the U2506 region in the samples from the U2585A and U2506G mutants, especially in the U2506G sample, where more than 50% of the crosslinking occurs in the U2506 region.

Although the preferential crosslinking of residue 2506 in the U2506G mutant may be due to the higher reactivity of guanine, another, more interesting interpretation of the preferential crosslinking to U2506 in the U2506G sample may be related to the model proposed by Schmeing and coworkers (**Figure 4B,** Schmeing et al., 2005). In this model, U2506, U2585 and the tRNA interact dynamically, and each nucleotide swings towards or away from the 3' end of P-site tRNA depending on the conformational state of the ribosome (Schmeing et al., 2005). During the transition state, when the peptide bond is forming, U2506 is close to the A76 of P-site tRNA. With a guanine at position 2506, U2506G may be fixed in a position adjacent to the 3' end of the P-site tRNA due to steric hindrance by the relatively bulky guanine, or due to the inability of guanine to form the wobble base pair with G2583 predicted by Schmeing et al., affecting the crosslinking pattern.

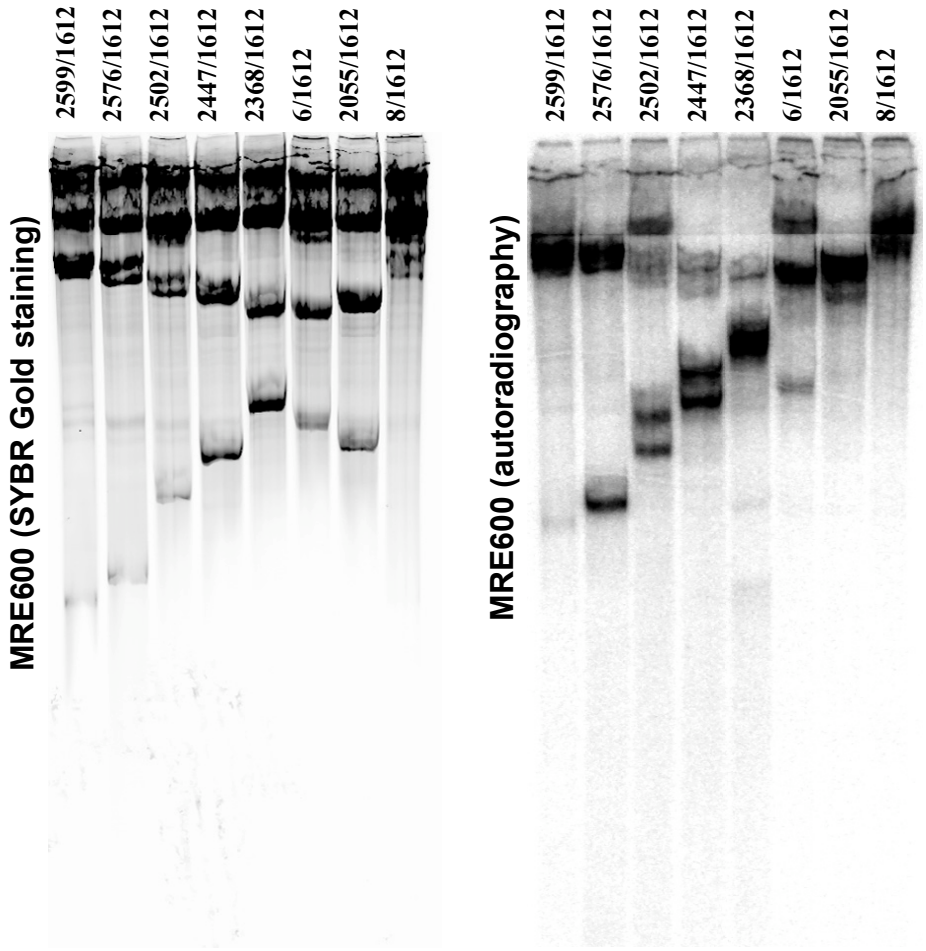

Figure 18. Analysis of tRNA-23S rRNA complexes by RNase H digestion using oligodeoxyribonucleotides and chimeric 2'-*O*-methyl/deoxyribonucleotides. 5% TTGP gels of RNase H-digestion products. Each sample was cleaved by RNase H at the site of oligonucleotide 1612 to produce a 5' fragment short enough to enter the gel, thereby facilitating a check for the completeness of digestion. A second cleavage was targeted by a specific chimeric oligonucleotide, whose identity is shown above the lanes. The level of radioactivity in each band was measured by phosphorimaging to determine the percentage of tRNA crosslinked to the various segments of the 23S rRNA.

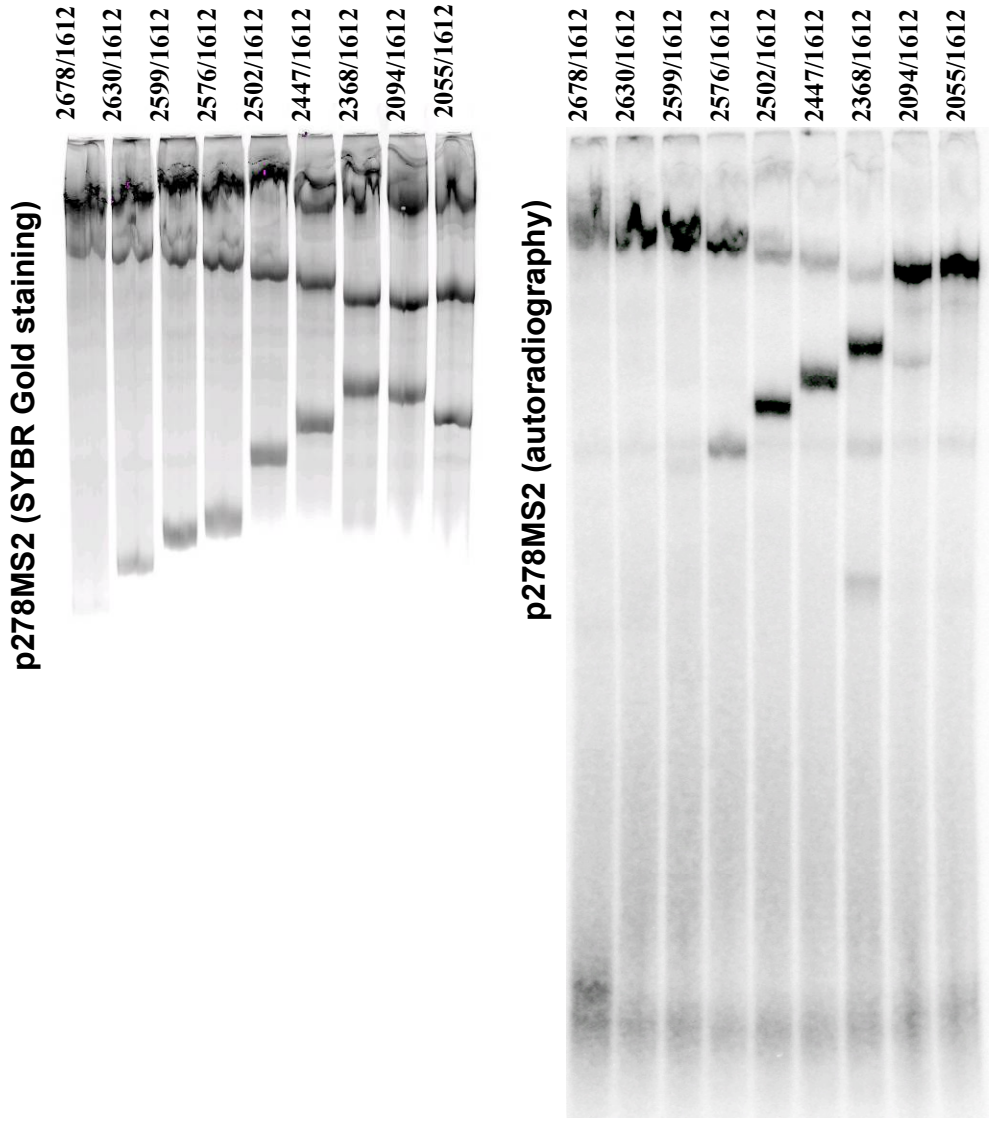
p278MS2 (SYBR Gold staining)
2678/1612
2630/1612
2599/1612
2576/1612
2502/1612
2447/1612
2368/1612
2094/1612
2055/1612
p278MS2 (autoradiography)
2678/1612
2630/1612
2599/1612
2576/1612
2502/1612
2447/1612
2368/1612
2094/1612
2055/1612

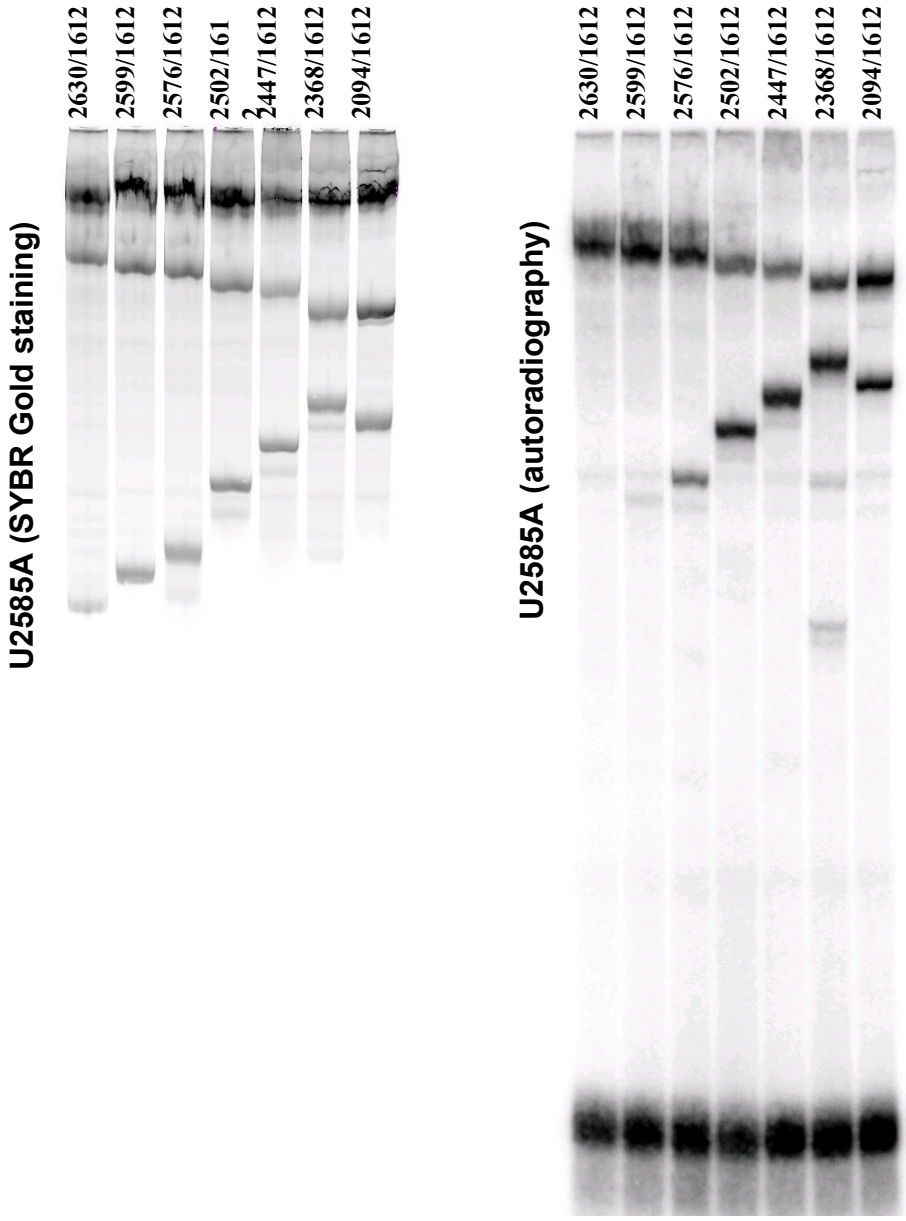
U2585A (SYBR Gold staining)
2630/1612
2599/1612
2576/1612
2502/161
2447/1612
2368/1612
2094/1612
U2585A (autoradiography)
2630/1612
2599/1612
2576/1612
2502/1612
2447/1612
2368/1612
2094/1612

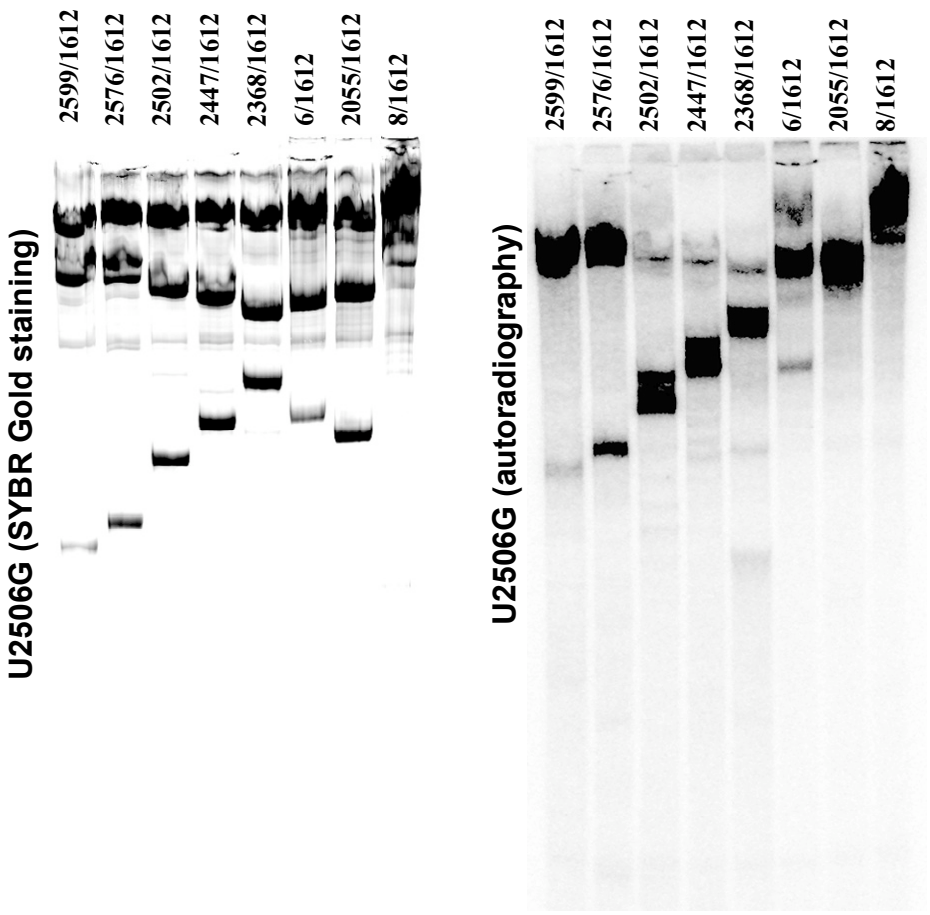
U2506G (SYBR Gold staining)
2599/1612
2576/1612
2502/1612
2447/1612
2368/1612
6/1612
2055/1612
8/1612
U2506G (autoradiography)
2599/1612
2576/1612
2502/1612
2447/1612
2368/1612
6/1612
2055/1612
8/1612

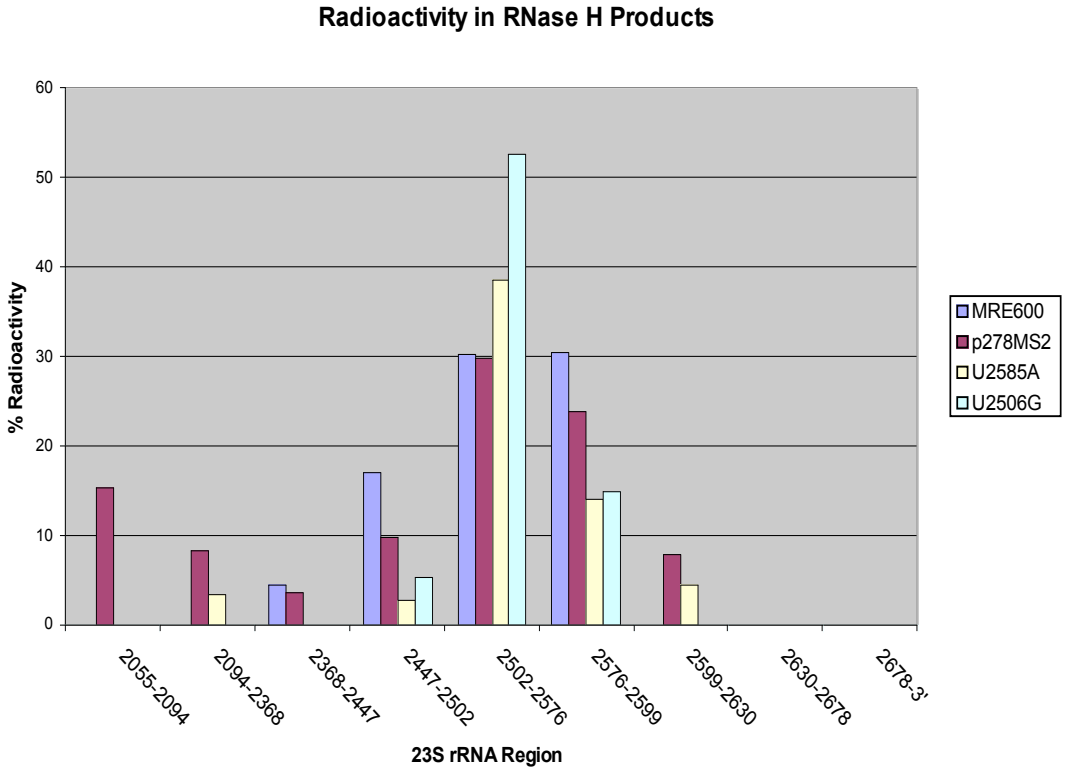

		% Radioactivity			
		MRE600	p278MS2	U2585A	U2506G
23S Region	2055-2094		15.4		
	2094-2368		8.4	3.5	
	2368-2447	4.6	3.7	0.0	0.0
	2447-2502	17.0	9.9	2.9	5.4
	2502-2576	30.3	29.8	38.7	52.7
	2576-2599	30.5	23.9	14.2	15.0
	2599-2630		7.9	4.4	
	2630-2678		0.0	0.0	
	2678-3'		0.0		

Figure 19. Localization of radioactivity to regions of 23S rRNA. The percent radioactivity in each region was calculated by subtracting the total radioactivity of RNase H products representing narrow regions from that of broader regions. For example, the percent radioactivity from 2576 to 2599 is equal to the total percent radioactivity in fragment "2599/1612" minus the total percent radioactivity in fragment "2576/1612." U2506G and p278MS2 values were based on the average of 2 and 3 trials, respectively. MRE600 and U2585A values were based on one trial. As indicated by the empty cells in the table above, all regions were not scanned in all cases due to the limited availability of material. Crosslinks are likely to occur in the vicinity of nucleotides 2585 and 2506, because of the high level of radioactivity that is present between oligonucleotides 2502 and 2576, and between 2576 and 2599. Additionally, the preliminary data suggest that, in the U2506G mutant, the ligand may crosslink preferentially to nucleotide U2506G relative to other crosslinking sites.

One problem that arose with this method is the appearance of some double bands in the radioactive scans that do not appear in the SYBR Gold staining pattern of the same gels. The double band only appears in the bands that correspond to fragments believed to contain two major crosslinks. One possible explanation is that each of the two bands corresponds to a different crosslink. Under the crosslinking conditions used in these experiments, each 23S rRNA strand can only be crosslinked to one tRNA molecule, because only one tRNA molecule may bind per 70S ribosome. Therefore a band that represents an RNase H fragment encompassing two crosslinking sites, a and b, will be comprised of two distinct crosslinked species; one with tRNA bound to site a, and one with tRNA bound to site b. tRNA covalently bound to different positions in the 23S rRNA could affect the branched shape of the fragment, resulting in different mobilities of the two species in the native gel.

Precise localization of 23S rRNA crosslinks: RNase H analysis helps to define general regions of crosslinking on the 23S rRNA but it is important to more precisely localize these sites by primer extension analysis. Because only a small percentage of the tRNA in the irradiated sample becomes crosslinked to 23S rRNA, the samples were first enriched for the crosslinked species. Fragments from 1612 to 2368 and 2369 to 3', which encompass all presumed crosslinking sites, were isolated by digesting crosslinked 23S rRNA with RNase H using oligonucleotides 1612 and 2368 (see Figure 7). When the digested samples were run on a gel, two SYBR Gold-dyed bands corresponding to the fragments 1612 to 2368 and 2369 to 3' were visualized. Two ^{32}P-labeled bands of interest with mobilities corresponding to fragments 1612 to 2368 and 2369 to 3' linked to

the 76-nt tRNA were also detected by autoradiography. These bands were excised and the rRNA fragments were purified.

Radioactively labeled primers 2667, 2579 and 2179 were used to analyze the purified crosslinked and non-crosslinked rRNA fragments by primer extension. The cDNA products were run on a sequencing gel and compared to a 23S rRNA sequencing ladder **(Figure 20)**. Under the conditions used, primer 2667 allows for the identification of crosslinks at the two primary nucleotides of interest, U2506 and U2585. Primer 2579 may also be used to identify U2506. Primer 2176 was used to scan a region further upstream of the PTC; however, the results of that experiment were difficult to interperet due to a high level of radioactive signal apparent in both the crosslinked and uncrosslinked control samples.

In each scan of the U2506 region, crosslinks at that nucleotide are found in the 23S rRNAs from all four test samples: MRE600, p278MS2, U2506G and U2585A **(Figure 20B)**. In scans of the U2585 region, 23S rRNAs from MRE600, p278MS2 and U2585A appear to be crosslinked to the 3'-end of P-site tRNA at nucleotide U2585 **(Figure 20C)**. However, during the two trials in which the U2506G mutant 23S rRNA was tested, there appears to be no crosslink at nucleotide U2585. These data are consistent with the RNase H data, which indicated preferential crosslinking of P-site tRNA to the U2506 region of the 23S rRNA, and a decreased level of crosslinking to the region of U2585, in the U2506G ribosomes.

Both the RNase H and the primer extension data for the U2506G ribosomes are consistent with the model in which U2506 breaks from its original wobble base pair with G2583 and swings towards the A76 of P-site tRNA, while U2585 simultaneously moves

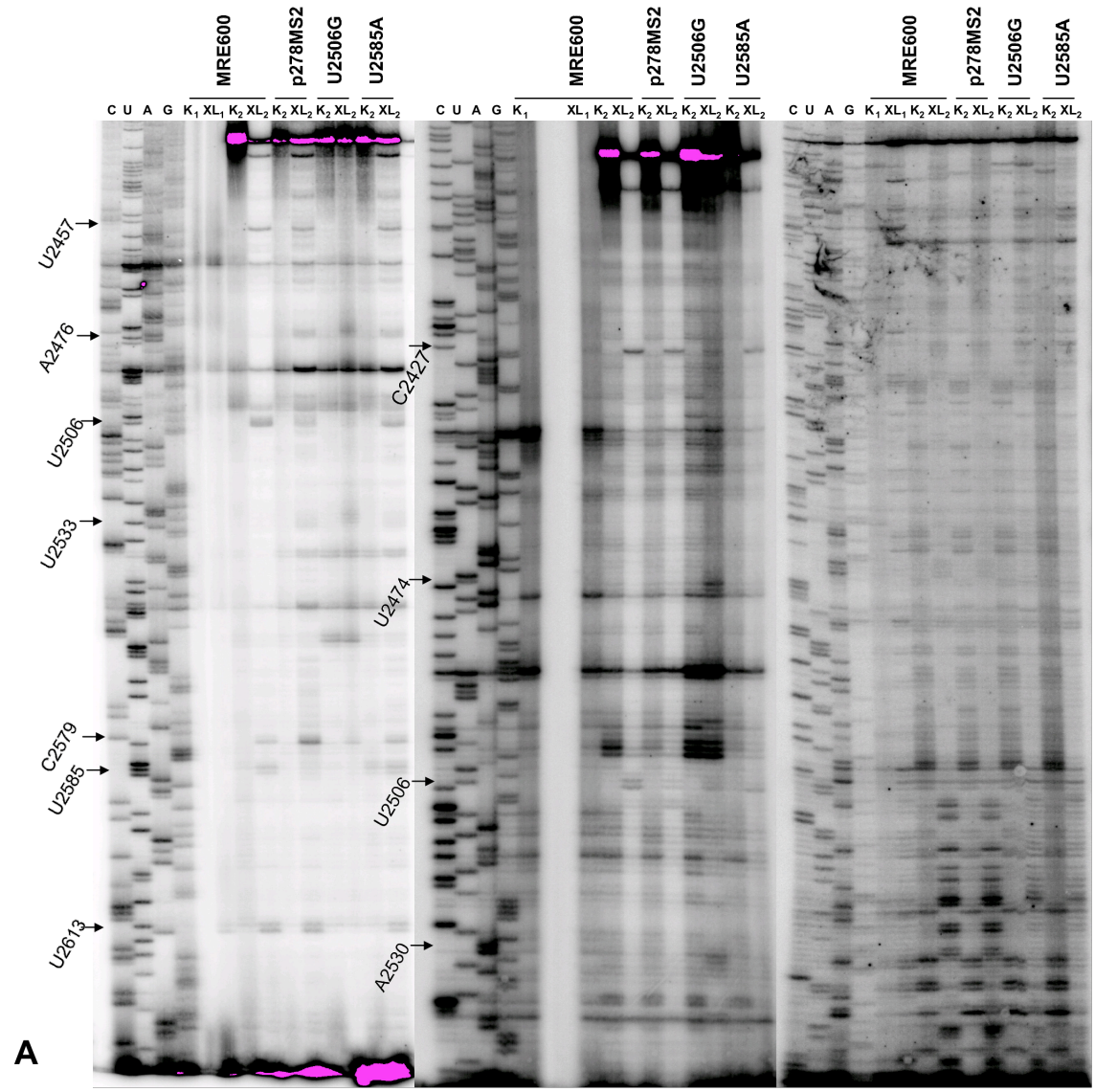

Figure 20. Primer extension analysis of crosslinked 23S rRNA. 6% polyacrylamide gels of primer extension products using primers 2667, 2579 and 2179. Lanes C, U, A, and G represent dideoxynucleotide sequencing ladders. Lanes labeled K_1 are full length, uncrosslinked MRE600 controls, and lanes labeled XL_1 are full-length, crosslinked MRE600 controls. Lanes labeled K_2 are the uncrosslinked fragments isolated from the RNase H digest of the crosslinked samples. Lanes labeled XL_2 are the crosslinked fragments isolated from the RNase H digest of the crosslinked samples. **(A)** Crosslinked sites are localized by comparing primer extension stops in the experimental lanes to the dideoxynucleotide sequencing ladder. **(B)** and **(C)** Enlargements of U2585 and U2506 regions of the sequencing gels using primers 2667 and 2579, respectively.

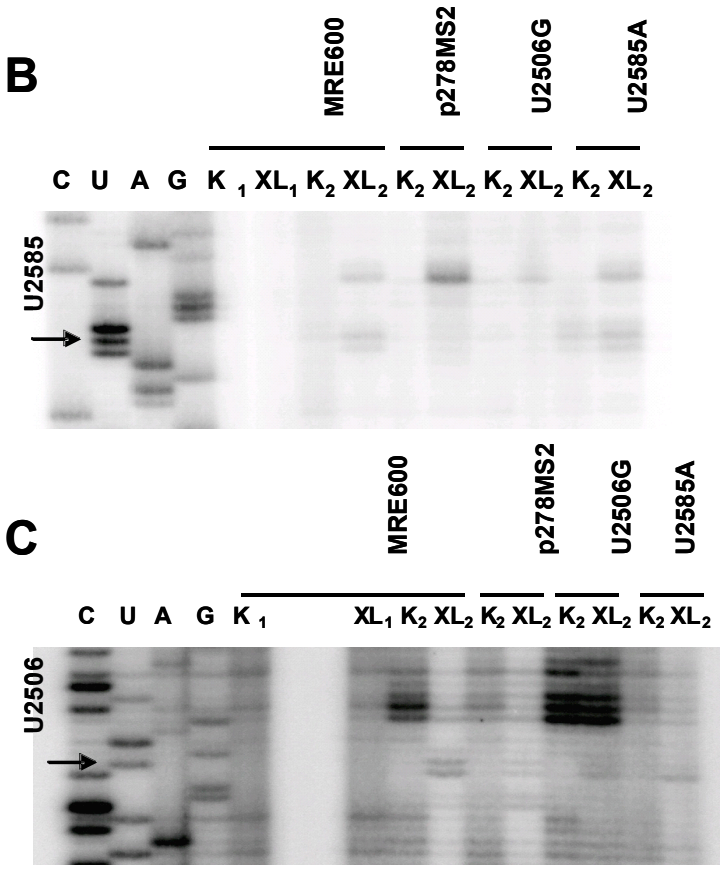
B
MRE600
p278MS2
U2506G
U2585A
C U A G K 1 XL1 K2 XL2 K2 XL2 K2 XL2 K2 XL2
U2585
C
MRE600
p278MS2
U2506G
U2585A
C U A G K 1 XL1 K2 XL2 K2 XL2 K2 XL2 K2 XL2
U2506

away from the A76 of P-site tRNA (Schmeing et al., 2005, Figure 4B). A G at position 2506 could not form a wobble base pair with G2583, and the bulkier G might remain adjacent to the 3' end of the P-site tRNA. In this situation, U2585 may be forced to remain in a position more distant from the A76 of the P-site tRNA where it is unable to become crosslinked. Furthermore, if U2585 remains in a position further away from the P-site substrate, U2585 will be unable to perform its duty to protect the P-site substrate from hydrolysis in the absence of an A-site tRNA, as expected in the model. In this situation, water could hydrolyze the peptidyl moiety, halting translation. This interpretation could explain the fatal nature of the U2506G mutation.

Additional crosslink sites were observed at nucleotides indicated in Figure 20. Most of the additional crosslink sites appeared in the control and test samples, suggesting that the mutations studied here do not alter the interaction of the 3'-end of the P-site tRNA with other regions of the PTC. One exception is the crosslink at position U2613, which occurs in both of the controls and the U2585A sample, but is not apparent in the U2506G sample. Another exception is the crosslinked region from A2530 to A2533. This region becomes crosslinked in the U2506G sample, but is not crosslinked in the controls or the U2586A sample. If confirmed by future experimentation, this could indicate other regions of the PTC that are involved in positioning the 3'-end of the P-site tRNA.

CHAPTER 4

DISCUSSION

The high-resolution crystal structure of the *H. marismortui* 50S subunit provides strong evidence that the 23S rRNA is the only catalytic entity in the peptidyl transferase center of the archaeal ribosome (Ban et al., 2000). In the bacterial ribosome, however, there is in addition to RNA, a protein, L27, at the PTC (Maguire et al., 2005, Selmer et al., 2006). Various mechanisms for the catalysis of peptidyl transfer have been proposed. The idea that has garnered the most attention suggests that the 23S rRNA, and possible L27, act to position the peptidyl- and aminoacyl-tRNAs for spontaneous peptidyl transfer and that chemical catalysis may play only a secondary role (Polacek et al., 2001).

Nucleotides A2451, U2506, U2585, and U2602 are universally conserved at the site of peptide bond formation (Ban et al., 2000). Based on the crystallographic evidence, and because mutagenesis at these sites severely impairs peptide bond formation (Green et al., 1997; Polacek et al., 2001; Thompson et al., 2001; Youngman et al., 2004), these nucleotides are thought to be involved in positioning the 3' ends of A- and P-site substrates. In this study, pure populations of ribosomes with either U2585A or U2506G mutations in the 23S rRNA were analyzed to test the hypothesis that substitutions at conserved nucleotides U2585 and U2506 in the PTC impair peptide bond formation by altering the position of the 3' end of P-site tRNA relative to the 23S rRNA.

Mutant and wild-type ribosomes were probed with ^{32}P-labeled [2N$_3$A76]tRNA^{Phe} to determine how the 3' end of tRNA interacts with the ribosomal proteins and 23S RNA at the PTC. The photoreactive substrate was bound and crosslinked to 70S ribosomes from MRE600, as well as from those with MS2 inserts and U2585A and U2506G

mutations. Several similarities between the data for wild-type and mutant ribosomes suggest that the substitution mutations have little effect on the binding and crosslinking of P-site tRNA to the ribosome (see Table 3). As the results varied across several distinct trials, however (Table 3), further investigation is needed to confirm this observation.

Previous studies have shown that $[2N_3A76]tRNA^{Phe}$ at the P site forms crosslinks to specific 23S rRNA nucleotides, as well as to proteins L27 and L33 (Maguire et al., 2005; Wower et al., 2000). The covalent tRNA-ribosome complexes formed with the wild-type and mutant ribosomes were analyzed to determine crosslinking characteristics. In one experiment, SDS-PAGE analysis revealed a difference in the distribution of crosslinks between protein and 23S rRNA in ribosomes carrying the U2506G mutation with respect to the other ribosomes studied (Figure 14). However, no other trials have supported these data, and some have even shown contradictory results; therefore no conclusions can be drawn.

To determine the distribution of ligand-protein crosslinking amongst the various ribosomal proteins, the RNA components of the crosslinked ribosomes were digested with S1 nuclease, and the labeled proteins were analyzed. Although proteins L27 and L33 are expected to be resolved by SDS-PAGE, they were not distinguished in these experiments for reasons that are unknown.

The sites of tRNA crosslinking in the 23S rRNA were investigated by a methodology involving partial localization by site-specific RNase H digestion of tRNA-23S rRNA complexes. Previous studies have shown that nucleotides U2585 and U2506 become crosslinked to P-site $[2N_3A76]tRNA^{Phe}$ (Wower et al., 2000). Results obtained by analysis of crosslinking to specific segments of the 23S rRNA produced by RNase H

digestion of complexes between 23S rRNA and a set of chimeric oligonucleotides have shown that crosslinks are likely to occur in the vicinity of nucleotides 2585 and 2506 (Figures 18 and 19). Additionally, the data suggest that, in the U2506G mutant, the ligand may crosslink preferentially to nucleotide U2506G relative to other crosslinking sites.

Crosslinking sites on the 23S rRNA were more precisely localized by primer extension analysis. In scans of the U2585 region, the 23S rRNA of ribosomes from MRE600, p278MS2 and U2585A appear to be crosslinked to the 3'-end of P-site tRNA at nucleotide U2585 (Figure 21B). However, there appears to be no crosslink at nucleotide U2585 in the 23S rRNA carrying the U2506G mutation. These data are consistent with the RNase H data, which indicated preferential crosslinking of P-site tRNA to the U2506 region of the 23S rRNA, and a decreased level of crosslinking to the region of U2585, in the ribosomes with a G at position 2506.

Both the RNase H and the primer extension data for the U2506G ribosomes are consistent with the model in which U2506 breaks from its original wobble basepair with G2583 during A-site tRNA binding and swings towards the A76 of P-site tRNA, while U2585 simultaneously moves away from the A76 of P-site tRNA (Schmeing et al., 2005, Figure 4B). With a U to G mutation of nucleotide U2506, the original wobble basepair does not form, and the bulkier U2506G may retain a position adjacent to the 3' end of the P-site tRNA. In this situation, U2585 may be forced to remain in a position distant from the A76 of the P-site tRNA where it is unable to become crosslinked. Furthermore, if U2585 remains in a position further away from the P-site substrate, U2585 will be unable to protect the P-site substrate from hydrolysis in the absence of an A-site tRNA

(Schmeing et al., 2005). In this situation, water would hydrolyze the peptidyl moiety, halting translation.

BIBLIOGRAPHY

Ban, N; Nissen, P; Hansen, J; Moore, P. B; and Steitz, T. A. The complete atomic structure of the large ribosomal subunit at 2.4 Å resolution. *Science* **2002**, *289*, 905-920.

Baranovsky, A. G., Matushin, V. G., Vlassov, A. V., Zabara, V. G., Naumov, V. A., Giege, R., Buneva, V. N., and Nevinsky, G. A. DNA- and RNA-hydrolyzing antibodies from the blood of patients with various forms of viral hepatitis. *Biochemistry (Moscow)* **1997**, *62*.

Green, R., Samaha, R.R. and Noller, H.F. Mutations at nucleotides G2251 and U2585 of the 23S rRNA perturb the peptidyl transferase center of the ribosome. *J. Mol. Biol*. **1997**, *265*, 40-50.

Hansen, J. L., Schmeing, T. M., Moore, P. B., and Steitz, T. A. Structural insights into peptide bond formation. *Proc. Natl. Acad. Sci. USA* **2002**, *99*, 11670-11675.

Korostelev, A., Trakhanov, S., Laurberg, M., and Noller, H. F. Crystal structure of a ribosome-tRNA complex reveals functional interactions and rearrangements. *Cell* **2006**, *126*, 1-13.

Kim, D. F., and Green, R. Base-pairing between 23S rRNA and tRNA in the ribosomal A site. *Mol. Cell* **1999**, *4*, 859-864.

Maguire, B. A., Beniaminov, A. D., Ramu, H., Mankin, A. S., and Zimmermann, R. A. A protein component at the heart of an RNA machine: The importance of protein L27 for the function of the bacterial ribosome. *Mol. Cell* **2005**, *20*, 425-435.

Nissen, P., Hansen, J., Ban, N., Moore, P. B., and Steitz, T. A. The structural basis of ribosome activity in peptide bond synthesis. *Science* **2000**, *289*, 920-930.

Polacek, N., Gaynor, M., Yassin, A., and Mankin, A. S. Ribosomal peptidyl transferase can withstand mutations at the putative catalytic nucleotide. *Letters to Nature* **2001**, *411*, 498-501.

Samaha, R. R., Green, R., and Noller, H. F. A base pair between tRNA and 23S rRNA in the peptidyl transferase centre of the ribosome. *Nature* **1995**, *377*, 309-314.

Schmeing, T. M., Huang, K. S., Strobel, S. A., and Steitz, T. A. An induced-fit mechanism to promote peptide bond formation and exclude hydrolysis of peptidyl-tRNA. *Nature* **2005**, *438*, 520-524.

Schuwirth, B. S., Borovinskaya, M. A., Hau, C. W., Zhang, W., Vila-Sanjurjo, A., Holton, J. M., and Cate, J. H. Structures of the bacterial ribosome at 3.5 Å resolution. *Science* **2005**, *310*, 827-834.

Selmer, M., Dunham, C. M., Murphy IV, F. V., Weixlbaumer, A., Petry, S., Kelley, A. C., Weir, J. R., and Ramakrishnan. Structure of the 70S ribosome complexed with mRNA and tRNA. *Science* **2006**, *313*, 1935-1942.

Spahn, C. M., Grassucci, R. A., Penczek, P., and Frank, J. Direct three-dimensional localization and positive identification of RNA helices within the ribosome by means of genetic tagging and cryo-electron microscopy. *Struc. Fold. Des.* **1999**, *7*, 1597-1573.

Sylvers, L. A., Wower, J., Hixson, S. S., and Zimmermann, R. A. Preparation of 2-azidoadenosine 3', 5'-[5'-32P]bisphosphate for incorporation into transfer RNA. Photoaffinity labeling of *Escherichia coli* ribosomes. *FEBS Letters* **1989**, *245*, 9-13.

Sylvers, L. A., and Wower, J. Nucleic acid-incorporated azidonucleotides: probes for studying the interaction of RNA or DNA with proteins and other nucleic acids. *Bioconjug. Chem.* **1993**, *4*, 411-418.

Szymanski, M., Barciszewska, M. Z., Erdmann, V. A., and Barciszewski, J. 5S ribosomal RNA database. *Nucleic Acids Res.* **2002**, *30*, 176-178.

Thompson, J., Kim, D.F., O'Connor, M., Lieberman, K.R., Bayfield, M.A., Gregory, S.T., Green, R., Noller, H.F. and Dahlberg, A.E. Analysis of mutations at residues A2451 and G2447 of 23S rRNA in the peptidyltransferase active site of the 50S ribosomal subunit. *Proc. Natl. Acad. Sci. USA* **2001**, *98*, 9002-9007.

Wower, J., Kirillov, S. V., Wower, I. K., Guven, S., Hixson, S. S., and Zimmermann, R. A. Transit of tRNA through the *Escherichia coli* ribosome: Crosslinking of the 3' end of tRNA to specific nucleotides of the 23S ribosomal RNA at the A, P, and E sites. *J. Biol. Chem.* **2000**, *275*, 37887-37894.

Youngman, E. M., Brunelle, J. L., Kochaniak, A. B., and Green, R. The active site of the ribosome is comprised of two layers of conserved nucleotides with distinct roles in peptide bond formation and peptide release. *Cell* **2004**, *117*, 589-599.

Youngman, E. M., and Green, R. Affinity purification of *in vivo*-assembled ribosomes for *in vitro* biochemical analysis. *Methods* **2005**, *36*, 305-312.

Yusupov, M. M., Yusupova, G. Zh., Baucom, A., Lieberman, K., Earnest, T. N., Cate, J. H. D., and Noller, H. F. Crystal structure of the ribosome at 5.5 Å resolution. *Science* **2001**, *292*, 883-896.